Application of structure-from-motion photogrammetry to quantify coral reef structural complexity change following a mass mortality event

by

Kevin Bruce
B.Sc. Honours, University of Hawai'i at Hilo, 2014

A Thesis Submitted in Partial Fulfillment
of the Requirements for the Degree of

MASTER OF SCIENCE

in the Department of Biology

University of Victoria

Supervisory Committee

Application of structure-from-motion photogrammetry to quantify coral reef structural complexity change following a mass mortality event

by

Kevin Bruce
B.Sc. Honours, University of Hawai'i at Hilo, 2014

Supervisory Committee

Dr. Julia Baum, Supervisor
Department of Biology

Dr. Rana El-Sabaawi, Departmental Member
Department of Biology

Dr. John Burns, Outside Member
University of Hawai'i at Hilo

Abstract

Hermatypic, or reef-building, corals (Order Scleractinia) are the foundation of coral reefs, providing a diversity of structurally complex habitats for the myriad species in these biologically diverse ecosystems. However, both local and global anthropogenic stressors threaten the persistence of these corals. For this thesis, thirty 16m^2 permanent photoquadrats at 10 shallow forereef sites around Kiritimati (Christmas Island, Republic of Kiribati) were monitored across a four-year study encompassing the 2015-2016 El Niño derived marine heatwave, and subsequent mass coral mortality event. Sites were exposed to either low, medium, or high levels of local anthropogenic disturbance. My objective herein was to examine the effects of a mass coral mortality event on reef structural complexity, from the end of the event to three years afterwards. To do so, I digitally quantified six metrics of structural complexity for each photoquadrat sampled across three resolution scales for each of the five expeditions. Plots from 2015, 2017, and 2019 were later annotated based on the morphological structure present. I found that while significant declines in multiple of habitat metrics occurred by the end of the heatwave, no further significant declines occurred thereafter. However, this trend was lost as resolution scale increased, indicating the trends seen in the habitat metrics at 1.0 cm were likely documenting the shift from live coral towards abiotic dominated reefs. Anthropogenic disturbance compounded the El Niño's effect, ensuring high disturbance sites had the lowest structural complexity values throughout the study. Lastly, live branching, tabulate, foliose, and submassive coral morphologies were found to be most closely associated with the different habitat complexity metrics. These results highlight the importance live coral structure has on reef structural complexity, illustrate the importance of model resolution when quantifying trends in structural complexity, pinpoint coral morphologies creating reef structural complexity, and further emphasize the need to limit the effects of local anthropogenic disturbance on coral reefs.

Table of Contents

List of Tables

List of Figures

Acknowledgements

A sincere thank you to Dr. Julia Baum for being an empowering and nurturing mentor who actively encouraged my scientific inquisition and furthered both my self-belief and scientific understanding exponentially. Her ability to lay down clear, concise instruction filled with words of encouragement and constructive criticism were always greatly appreciated and have propelled me forward towards the science career I had always dreamed of. In addition to Julia, this project would not have been possible without Dr. John Burns. His valuable insight into the world of photogrammetry was instrumental in the completion of this project. A special thank you to Kailey Pascoe for answering the myriad of technical questions I had throughout the 3D modelling process and for hosting me in your house during my in-situ training in June 2019. We have both come a long way from those scientific diving days at UH Hilo, and I'm excited to see what the future in the world of marine ecology has in store for the both of us. Lastly, thank you to Dr. Rana El-Sabaawi for providing valuable insight during my committee meeting.

Christmas Island is a magical location and will always hold a special place in my heart. With that said, I never would have had the chance to travel there had I not had some valuable friends and mentors along the way. First, thanks to Mauritius Valente Bell (aka the "Most Valuable Braddah") who taught the scientific diving course I took while in Hawai'i that initially sparked my interest in conducting underwater research. Next, a huge thank you to my friend Kristina Tietjen, who gave me my first opportunity conducting scientific diving research on Christmas Island back in 2017. Thank you for the guidance and leadership you showed while on the past Kiritimati expeditions (2017-2019) I've been fortunate to be a member of. Without you giving me that opportunity, I know my life would be very different today and I can't thank you enough for that. While the work is hard and the hours are long, I never stopped enjoying myself and was always amazed at the beauty Christmas Island possessed. In that same breath, I want to thank Julia again for taking a chance on me and trusting in Kristina's judgement. Next, it would be remiss to not acknowledge and deeply thank all past and present Kiritimati research crews, whose hard work and long hours under the Christmas Island sun have enabled the scope of this project to be so large. Lastly, thank you to the people of Christmas Island, who opened their doors to their little piece of paradise and allowed the research to be conducted on their home reefs they rely so dearly on. I will forever cherish the memories of the fieldwork, outreach with the local school children, and general island living during these expeditions.

Back in Victoria, I had a wonderful professional support network from everyone within the Baum and Juanes lab groups. Thanks for all the laughs, assistance, and words of encouragement throughout the past two years. From lunchroom discussions to road trips to PEEC, you all helped me to temporarily escape the stressful grad student life and enjoy the moment filled with hearty laughs and big smiles. A special shout-out to Dom, Kristina, and Sean who all spent far too many hours assisting me with my seemingly endless coding issues. Your patience was, and continues to be, so greatly appreciated! Furthermore, I'd like to offer a heartfelt thank you to all the undergraduate volunteers who assisted on this project. Brittany, Lydia, and Nathan: thank you for your diligence, patience, and attention to detail during the many hours of monotonous benthic structure tracing this study required!

A sincere thank you to the funding sources that allowed me to conduct my research: Mitacs Accelerate Fellowship, University of Victoria Centre for Asia-Pacific Initiatives, and the

UVic Faculty of Graduate Studies. Additional thanks to both Rob and Tammy Lipson and the family of Greig Cosier, who all provided greatly appreciated scholarships throughout my two years at UVic. Lastly, thanks to the many funders of Kiritimati fieldwork, whose support makes this study possible, that include: University of Victoria, the Natural Sciences and Engineering Research Council of Canada (NSERC), the National Science Foundation, The Rufford Maurice Laing Foundations, the Canadian Foundation for Innovation, the Packard Foundation, the Pew Charitable Trusts, National Geographic, and the Government of Kiribati.

And last, but most certainly not least, I can’t thank my family enough for all the love and support they have provided both throughout the degree. For the past 29 years, my parents have been nurturing my inquisitive spirit and encouraging me to pursue a career I feel I can make the biggest difference in.

Dedication

"An understanding of the natural world, and what's in it, is a source of not only a great curiosity, but great fulfilment." – David Attenborough

To my family, for inspiring my curiosity and nurturing my inquisitive nature from a young age, both of which have brought me along my path to where I am today.

Chapter 1- Introduction

Habitat complexity has long been associated with ecosystem productivity as the abiotic and biotic structures influence organismal species richness and abundance within ecosystems worldwide (MacArthur and MacArthur 1961; August 1983; Wilson et al. 2006; Alvarez-Filip et al. 2015). The magnitude of habitat complexity present at a location is typically determined by morphological attributes and local abundances of the ecosystem engineers present (Couch et al. 2017), with more complex growth forms deriving higher complexity values (Kovalenko et al. 2012; Burns et al. 2016). Ecosystem engineers physically shape the environment (Jones et al. 1994) and may also act as foundation species within the ecosystem by controlling ecosystem dynamics and influencing local and regional biodiversity (Ellison 2019). Species constructing a complex array of structure within the ecosystem create a wide-range of microhabitats to be utilized (MacArthur and MacArthur 1961; Friedlander and Parrish 1998; Kostylev et al. 2005), thereby allowing a higher diversity of organisms to exist in the area, particularly in prey species who use the array of structure in predator-avoidance measures (Finstad et al. 2007).

This concept of increased structure leading to additional niche space availability is prevalent across many terrestrial ecosystems (MacArthur and MacArthur 1961; August 1983; Lassau et al. 2005; Ghadiri Khanaposhtani et al. 2012). Perhaps the most influential study that first approached habitat complexity and its implications on diversity was MacArthur and MacArthur (1961)'s research, which found that areas of forests exhibiting higher habitat complexity offered additional niches for organisms to fill, which enabled bird species diversity to increase in the area. Forest ecosystem diversity goes beyond just birds however, as forests provide multiple tiers of complexity, opening up niches for mammals (August 1983) and birds

(MacArthur and MacArthur 1961) to occupy within the canopy, with the leaf litter providing a diverse range of non-homogeneous microhabitats available for smaller organisms to inhabit (Lassau et al. 2005; Ghadiri Khanaposhtani et al. 2012). Structural complexity of the ecosystem can also impact predator-prey dynamics, as seen in Australian feral cat populations where more structurally-complex environments inhibited invasive predators (Hohnen et al. 2016), and lowered predation success rates (McGregor et al. 2015).

Within marine ecosystems, habitat complexity (also termed structural complexity) is extremely important and dictated by the physical structure of the ecosystem engineer present, most notably in coral and kelp-dominated ecosystems (Ferrari et al. 2016; Filbee-Dexter and Wernberg 2018). Dominant in many temperate marine environments (Mann 1973; Dayton 1985), kelps originate on the seafloor and grow upwards towards the light, with the sheer mass of kelps able to dampen wave surge, shade sections of the seafloor, and provide complex habitat refuge space for a myriad of marine organisms throughout the tiered levels of the kelp (Mann 1973; Steneck et al. 2002; Steneck and Johnson 2013; Teagle et al. 2017). Both seagrass and mangroves drive their respective ecosystem's complexity, which is vitally important during the early lifecycle of many fish species (Dorenbosch et al. 2005; Henderson et al. 2017). Hard corals are the tropical counterpart to kelp, commonly occur in shallow, oligotrophic tropical waters, and provide the foundation of coral reef ecosystems (Burns et al. 2015a). In the absence of corals, the structurally complex habitat required by the wide-range of reef-inhabiting organisms wouldn't be available and the ecosystem would negatively suffer, as seen in the flattening of the reefs in the Caribbean over the past 40 years (Alvarez-Filip et al. 2009).

1.1 Coral Reef Structural Complexity

In tropical coral reef ecosystems, hermatypic corals (order Scleractinia; 'hard corals') act as the foundation species that physically engineer the structure of the reef and through doing so, provide the many microhabitats filled by countless organisms (Couch et al. 2017). Structural complexity of coral reefs is defined as the physical three-dimensional (3D) structure of the reefscape, primarily created by these hard corals (Luckhurst and Luckhurst 1978; Bellwood et al. 2004; Graham and Nash 2013; Bozec et al. 2015; Burns et al. 2015a), however other reef inhabitants contribute towards reef structure, including sponges, tubeworms, molluscs, and a variety of algal species (Hoegh-Guldberg 1999). Hard corals are capable of building calcareous structure beneath each polyp through the secretion of aragonite derived from the algal symbiont (*Symbiodinium spp.*) living within the coral's tissues, which provides up to 95% of the coral's metabolic requirements via photosynthesis (Hoegh-Guldberg et al. 2007; Burns et al. 2015a). Inter- and intra-specific competition for space and light has caused coral morphological growth forms to develop in a broad range of forms (Stoddart 1969; Todd 2008). Diversity in coral morphology occurs through competition for space and sunlight as coral colonies along the reef grow closer together (Vermeij 2006). This heterogeneity of coral growth forms allows coral reefs to provide a wide range of microhabitats for reef reliant organisms to inhabit, and it is this habitat diversity that enables coral reefs to be the most biodiverse marine ecosystem on the planet (Risk 1972; Luckhurst and Luckhurst 1978; Hughes et al. 2003; Alvarez-Filip et al. 2009).

While the principle structure of coral reefs is comprised of biotic components, abiotic structure also comprise portions of natural reef habitat (Burns et al. 2015a). Sand patches and rubble fields are natural components to reef ecosystems, with the latter providing habitat preferred by crypto-benthic fishes (Depczynski and Bellwood 2004), crustaceans (Kramer et al.

2014), and free-living corals (Hennige et al. 2017). If reefs are comprised of high rubble cover, coral settlement and recovery may be hindered as rubble and other loose material provide poor locations for larvae to recruit to and survive on to adulthood (Mumby et al. 2007; Chong-Seng et al. 2014). Many juvenile corals that recruit to these "killing fields" of coral rubble end up being heavily damaged or killed as the unattached rubble moves during high surge conditions (Fox et al. 2003; Ceccarelli et al. 2020). Due to this, stabilization of the rubble through support mesh, netting, or cement is often used on reef restoration projects (Boström-Einarsson et al. 2020; Ceccarelli et al. 2020). However, this can be an expensive process which may not be viable in remote countries lacking financial support (Haisfield et al. 2010). As climate change-induced mass coral mortality events increase, the ratio of living coral to dead coral rubble is expected to decrease, thereby confounding the issue by creating more of the "killing fields" (Perry and Alvarez-Filip 2018; Ceccarelli et al. 2020). Additionally, man-made artifacts (ex: shipwrecks, anchors) find their way onto the seafloor and may provide suitable substrate to allow for future coral settlement and recovery, however they often begin life on the reef in a structurally destructive manner (Harriott and Dinsdale 2004; Simon et al. 2013; Ceccarelli et al. 2020).

Coral reefs are constantly being eroded through physical, chemical, and biological forces (Hutchings 1986). Tropical storms produce strong surge and wave energy that can cause severe structural damage, as seen with cyclone Nathan causing a reported 90% decline in coral cover on the GBR in 2004, which left the majority of corals present as shattered debris littering the seafloor (Baird et al. 2018). Frequent strong wave surge has the ability to alter species composition, favoring reef composition in these areas towards species possessing morphological traits that enable higher resilience to wave surge (Stoddart 1969; Chappell 1980). Chemical dissolution of coral structure occurs frequently by a host of organisms, from microscopic fungi and foraminfera to larger invertebrates such as various worm, shrimp, and mollusc species (Glynn 1997), and through global climate change induced ocean acidification (Hoegh-Guldberg et al. 2007; Fabricius et al. 2014). Physical excavation of structure is a continual event on coral reefs, primarily done through bioeroding echinoids and herbivorous fishes, yet these commonly do not overcome coral accretion on established reefs (Glynn 1997; Bellwood et al. 2004). However, disturbance events can change this equation. For example, mass mortality events act as a catalyst causing significant changes in reef structure, as the physical, chemical, and physical erosional processes of the reef overtake coral accretion rates and work to break down the recently deceased coral skeletons (Hoegh-Guldberg 1999). This is particularly prevalent for large populations of both echinoids and herbivorous fishes, both of which can cause large amounts of structural damage to the dead coral structure by foraging for the algae recently colonized to the reef following the mass mortality event (Bellwood and Choat 1990; Bozec et al. 2015).

1.1.1 Ecological Importance of Coral Reef Structural Complexity

High levels of reef structural complexity have been attributed to influencing a host of processes on coral reefs, with the relationships between reef structure and fish abundance and diversity the most studied (Luckhurst and Luckhurst 1978; Jones et al. 2004; Wilson et al. 2007; Graham and Nash 2013; Bozec et al. 2015). In general, an increase in reef habitat complexity and morphological heterogeneity often leads to increased reef fish species richness (Gratwicke and Speight 2005b; Wilson et al. 2007), however the strength of the relationship varies based on location and species present (Luckhurst and Luckhurst 1978; Bozec et al. 2015). As a significant portion of reef inhabitng fishes reside close to or within the substrate provided by the corals (Pratchett et al. 2011; Darling et al. 2017), varying levels of structural complexity will impact their abundance and diversity due to their reliance on the habitat structure for predator avoidance, shelter, and possibly as a food source (Luckhurst and Luckhurst 1978; Warfe and Barmuta 2004; Gratwicke and Speight 2005b; Finstad et al. 2007) Variability in the available habitat structure present allows for a diverse range of juvenile fish to settle across the reef, as these juvenile fishes often prefer to settle in areas with refuse spaces shaped similar to their own body sizes (Hixon and Beets 1993). Losses in coral cover negatively impact these structure-dependent fishes, as seen by Jones et al. 2004 who discovered that more than 75% of all fish populations inhabiting their studied coral reefs around Papua New Guinea significantly reduced in numbers following a severe loss in coral cover, indicating the fish's reliance on the corals for settlement, shelter, and food. Corallivorous fishes, a distinct functional group of tropical fishes found on coral reefs that rely on coral tissue for sustenance (Pratchett 2005; Cole et al. 2008), are often disproportionately impacted by the loss of coral structure. This is particularly true for the fishes classified as obligate corallivores, as they rely primarily on corals as their main food source, rather than their facultative counterparts that are able to shift to alternative food sources in times of high coral mortality (Harmelin-Vivien and Bouchon-Navaro 1983; Cole et al. 2008; Graham et al. 2009).

1.1.2 Methods for Quantifying Coral Reef Structural Metrics

Coral reef studies of the past pioneered the quantification of structural complexity in aquatic systems, with recent breakthroughs the past decade in geomatics technology allowing scientists to push through previous limitations in coral reef structural complexity studies (Westoby et al. 2012). A variety of past methods have been used to quantify various attributes of reef complexity, known as reef rugosity (Alvarez-Filip et al. 2009). Simple and inexpensive fine scale measurements were often conducted using the chain-tape method, where divers take a chain with specific sized links and drape it over the reef substrate (Fig. 1.1) to compare the contour distance verses the linear distance the chain covers (Risk 1972; Hill and Wilkinson 2004; Friedman et al. 2012). Alternatively, trained technicians can visually assign a habitat assessment score (HAS) to a patch of reef (Polunin and Roberts 1993; Wilson et al. 2007). Broader, more expensive surveys used to digitally map larger areas of seascape utilizing Light Detection and Ranging (LIDAR) and Sound Navigation and Ranging (SONAR) technology have also been used in the past (Storlazzi et al. 2016). While all methods are applicable for benthic seafloor measurements, each has its own unique drawbacks. While simple and inexpensive, the chain-tape method has been shown to present imprecise predictions of structural complexity through haphazard chain placement, produce imprecise reports across multiple diving technicians, technicians, possess replicability issues through incorrect chain placement, and has the potential of damaging the coral substrate (Knudby and LeDrew 2007; Friedman et al. 2012; Dustan et al. 2013). Habitat assessment scores (HAS) form a qualitative method to obtain rugosity values that are incredibly quick and easy to obtain (Gratwicke and Speight 2005b; Wilson et al. 2007), however these values coarsely summarize habitat complexity across the entire site and limit the ability to conduct future analyses (Harborne et al. 2012). SONAR and LIDAR provide fine scale geophysical maps of the substratum depth (Costa et al. 2009), however financial restrictions (Delparte et al. 2014; Javernick et al. 2014) have limited their use to date to studies with cheaper alternatives available.

Figure 1.1 The chain-tape methodology illustrated showing how the contour distance of the chain (L_{chain}) is compared with the linear distance of the chain (D_{chain}) to determine a value of reef structural complexity (rugosity). Reported by Friedman et al. 2012, with figure adapted from Hill and Wilkinson 2004

The limitations of past methods attempting to quantify reef structure, combined with recent computer technology advancements, have led to the development of Structure-from-Motion (SfM) photogrammetry, which aims to increase the robustness and precision of the data collected while remaining financially feasible for the majority of researchers (Westoby et al. 2012; Burns et al. 2016). The process of SfM follows the same rules as stereoscopic photogrammetry in that a series of overlapping images (Fig. 1.2) of the reefscape are superimposed on one another to create a three-dimensional (3D) model of the reef (Westoby et al. 2012; Burns et al. 2015a). SfM is becoming a more well-used method for remote fieldwork examining reef structure due to its low-cost, user-friendly capabilities that enable increased sampling of an area due to decreased field processing time underwater (Westoby et al. 2012; Fukunaga et al. 2019a). In doing so, researchers can further focus on collecting more data during the research expeditions and rely on powerful computer programs to quantify benthic terrain measurements of reef habitat structure, at either a meso- or micro-scale, once back in a laboratory setting (Westoby et al. 2012; Burns et al. 2016).

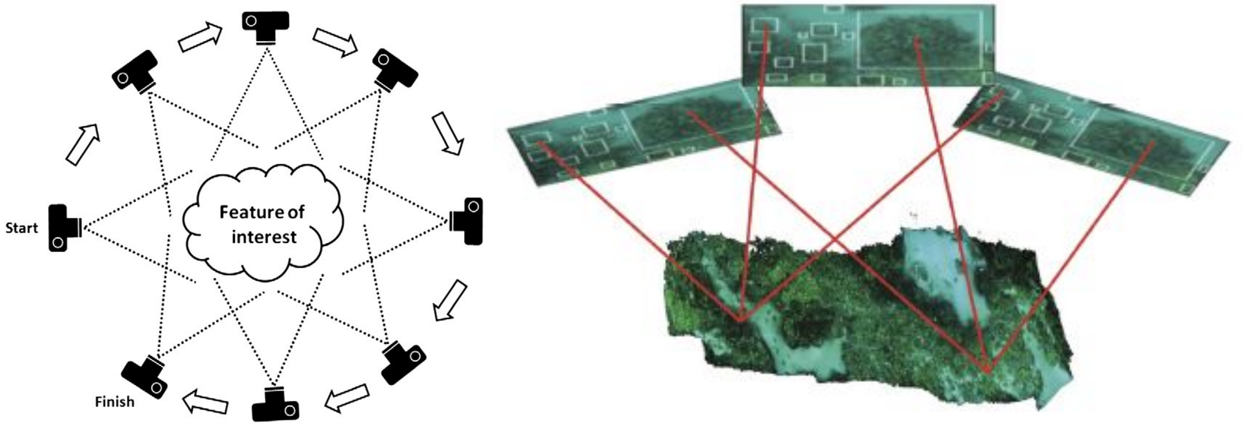

Figure 1.2 Steps involved in image collection and creation of the 3D models used in SfM Photogrammetry. A collection of images (left) from all angles around the subject are taken (Westoby et al. 2012) which are later aligned (right) and stitched together in the computer program to create the 3D model (Burns et al. 2015a).

1.2 Global stressors facing coral reefs

Coral reefs are threatened globally by multiple aspects of climate change, most notably through increases in ocean temperatures and marine heatwaves (short-lived temperature anomalies), and ocean acidification (Eakin et al. 2016; Frölicher and Laufkötter 2018; Oliver et al. 2021). Increases in global mean sea temperature (GMST) have occurred over the past century (Hoegh-Guldberg 1999) and are proving cause for concern, however the greatest threat to coral reefs the past few decades has been marine heatwaves (Eakin et al. 2016; Leggat et al. 2019). Defined as "periods where daily temperatures were reported at levels exceeding the seasonally varying 90th percentile threshold for at least five consecutive days" (Oliver et al. 2018), marine heatwaves (MHWs) have caused severe disturbance events to marine ecosystems (Couch et al. 2017; Hughes et al. 2017; Leggat et al. 2019; Magel et al. 2019). In order to track and prepare for these marine heatwaves, NOAA Coral Reef Watch (CRW) has devised a bleaching alert system which breaks up the ocean surface into 5km cells and classifies each region's risk of coral bleaching based on whether specific criteria are met involving temperature hotspots (positive-only temperature anomalies in the area which can cause initial bleaching) and Degree Heat Weeks (which is a useful predictor of coral bleaching that documents the accumulated thermal stress corals in the area have faced over a 12-week period) (Liu et al. 2014). Degree Heat Weeks (DHW) are calculated by adding any hotspots of 1 °C or greater within the past 12-week period together to create a running total of accumulated thermal stress in the area (Liu et al. 2014), with these values able to compound in times of severe heat stress. For example, two DHWs is equivalent to either two constant weeks of anomalous SST at 1 °C or one week of anomalous 2°C (Kayanne 2017). Based on these DHW values, the CRW has been able to create a bleaching alert criteria whereby at Bleaching Alert Level 1 (1 or more hotspots and anywhere between 4 to less than 8 DHW) coral bleaching is likely and at Bleaching Alert Level 2 (1 or more hotspots and 8 or more DHW) coral mortality is likely (Liu et al. 2014). Lastly, changes in the global climate are causing reef-damaging tropical storms to occur and cause severe damage on both reefs and the nearshore coastlines (Hoegh-Guldberg et al. 2019), with predictive modelling forecasting these storms to become more frequent and severe as we progress through the Anthropocene (Hughes et al. 2018a; IPCC 2019).

Coral bleaching is a phenomenon caused by environmental stressors and has been shown to negatively impact corals (Glynn 1983; Loya et al. 2001; Leggat et al. 2019). Initially documented by Glynn (1983), bleaching of the coral’s tissue has since been shown to occur from prolonged exposure to altered environmental conditions, such as altered salinity (Rogers 1990), increased UV radiance (Brown 1997), and increased sedimentation (Rogers 1990). However, increases sea surface temperature (SST) is the most common stressor causing corals to bleach

(Hoegh-Guldberg 1999). During a bleaching event, coral polyps physically expel the symbiotic algae from within its tissues, thereby limiting its nutrient uptake, hindering growth, and lowering resilience to future disease and bleaching events (Heron et al. 2016; Couch et al. 2017). If elevated SST's persist, coral mortality is likely, with the degree to which mortality occurs being proportional to the duration and extent of the elevated temperatures (Hoegh-Guldberg 1999). Mass bleaching and subsequent mortality events leave the reef vulnerable to significant structure loss through dissolution of dead calcareous structure (Leggat et al. 2019), increased bioerosion rates from herbivorous species (Glynn 1997), and physical damage from anthropogenic (Leggat et al. 2019) and climatic (Hoegh-Guldberg et al. 2019) sources.

Global climate change induced marine heatwaves have led to significant mass coral bleaching events in the past few decades (Brown 1997; Graham and Nash 2013; Heron et al. 2016; Magel et al. 2019). Reefs in the Caribbean Sea (Alvarez-Filip et al. 2009), Pacific Ocean (Magel et al. 2019; Vargas-Ángel et al. 2019), Indian Ocean (Graham et al. 2009), Hawai'i (Couch et al. 2017) and the Great Barrier Reef (Hughes et al. 2017) have all experienced the mass bleaching events derived from marine heatwaves. Alvarez-Filip et al. (2009) documented drastic losses in reef complexity throughout the Caribbean over the past 40 years, with disease and mass bleaching events driving the losses seen over time. Hughes et al. (2017b) examined repeated mass bleaching events occurring in 1998, 2010, and 2015/16 along the great barrier reef in Australia, noting that each subsequent bleaching event experienced increased proportions of bleached corals than previous events and the lack of disparity on which corals bleached, with neither age nor size providing added resilience to bleaching. Of all marine heatwaves the past few decades, the 2015-2016 El Niño-induced marine heatwave caused previously unprecedented ecological consequences worldwide, including at locations previously untouched by past marine heatwaves (Eakin et al. 2016). This particular heatwave also forced several reefs to reach a previously-unprecedented 24 DHWs, surpassing the hypothesized threshold of these heatwaves set less than a decade prior (Hoegh-Guldberg 2011). Even remote reefs weren't spared, with widespread mass bleaching events occurring in the central equatorial Pacific Ocean (Kiritimati, Republic of Kiribati) and the northwestern Hawaiian islands within the past 4 years (Couch et al. 2017; Magel et al. 2019).

Additional climate change derived stressors facing coral reefs include ocean acidification and increased severity of tropical storms via altered climatic patterns (Fabricius et al. 2014; Baird et al. 2018; IPCC 2019). Ocean acidification, a process where increased carbon dioxide uptake by the oceans is causing the pH levels to drop, is increasing the rates of dissolution of calcareous structures in a host of marine organisms, including corals, shellfish, and multiple genera of phytoplankton (Hoegh-Guldberg et al. 2007; Doney et al. 2009; Talmage and Gobler 2010). Increased water acidity causes coral growth rates to slow as colony growth is offset by increased dissolution of carbonate structure (Hoegh-Guldberg et al. 2007). Additionally, changes in the global climate are causing reef-damaging tropical storms to occur and cause severe damage on both reefs and the nearshore coastlines (Baird et al. 2018; Hoegh-Guldberg et al. 2019), with predictive modelling forecasting these storms to become more frequent and severe as we progress through the Anthropocene (Hughes et al. 2018b; IPCC 2019).

1.3 Local stressors facing coral reefs

Beyond climate change, coral reefs are also threatened by a suite of local anthropogenically-derived disturbances, including overfishing (Wilson et al. 2010), pollution (van den Brink et al. 2011), eutrophication (Sebens 1994), sedimentation (Hoegh-Guldberg 1999), disease (Lamb et al. 2014), and physical destruction (Harriott and Dinsdale 2004; Lamb et al. 2014). Habitat alteration and damage to the reef structure via destructive fishing methods and boat anchors are causing major structural alterations to reefs (Reed et al. 2007; Pratchett et al. 2011), with both bottom trawling and dynamite fishing practises having the ability to cause near 100% coral mortality when used (Raymundo et al. 2007; Reed et al. 2007). Even if the coral colony escapes complete destruction, any level of physical damage to the corals skeleton opens up pathways for disease to enter coral tissue and can potentially lead to mortality later in the future (Dinsdale and Harriott 2004; Lamb et al. 2014). Ecosystem processes and trophic chains preventing macroalgal phase-shifts can be altered through overfishing a single species of fish (Roberts 1995). Terrestrial runoff from golf-courses, agriculture, and improper land use/portioning causing erosion of river banks are causing cause coral mortality through the processes of eutrophication (Sebens 1994; Dubinsky and Stambler 1996), sedimentation (Hoegh-Guldberg 1999), and pollution (van den Brink et al. 2011). Eutrophication, sedimentation, and pollution can all act additively or synergistically upon one another, with increased offshore water discharge able to cause coral mortality through suffocating the corals in sediment (Hoegh-Guldberg 1999) or by creating anoxic patches on reefs by stimulating oxygen-consuming microbes within the water column (Dubinsky and Stambler 1996). Excess pollutants can also make their way to the reef through this offshore discharge and have the ability to both induce eutrophication and lower coral resilience to future stressors (van Dam et al. 2011).

1.4 Thesis Research

This thesis looks to further our understanding on the effects that local and global stressors have on reef habitat structural complexity. Specifically, I 1) examined the effects of a severe heat stress event and local anthropogenic disturbance on habitat structural complexity, 2) investigated the impact resolution scale has on the habitat metrics, and 3) highlighted key morphological drivers of each habitat metric. Data for this study was collected from around Kiritimati (Republic of Kiribati), a remote coral atoll in the central equatorial Pacific Ocean severely impacted by the 2015-2016 marine heatwave, which also has a natural gradient of local anthropogenic disturbance present across the atoll (Watson et al. 2016). As this was the most severe marine heatwave on record (Claar et al. 2018) that decimated the coral communities surrounding Kiritimati (Baum et al., *in prep*), I anticipated I would be documenting the continual degradation of coral reef structural complexity through time as the coral structure eroded further. With local anthropogenic disturbance further compounding the heatwave's effects, I hypothesized that sites experiencing higher local anthropogenic disturbance would consistently report the lowest structural complexity values. Additionally, I predicted that trends seen in the habitat metrics would change based on the resolution scales used to quantify them, as previous studies examining these metrics at different resolutions found similar results (Fukunaga et al. 2020a; Fukunaga and Burns 2020). Lastly, I predicted that the corals historically labelled as being complex (Loya et al. 2001; Gates and Ainsworth 2011; Graham and Nash 2013), such as the branching and tabulate morphologies, would be highlighted as key predictors for the habitat metrics of complexity whereas larger massive and submassive morphologies will be key predictors for the curvature metrics as these were found to better explain the underlying reef substrate than the intricate complexity values on coral reefs (Fukunaga et al. 2020a).

In Chapter 2, I utilized Structure-from-Motion (SfM) photogrammetry to characterize reef habitat structure around Kiritimati (Republic of Kiribati) and examine the effects both the marine heatwave and local anthropogenic disturbance had on reef structural complexity across a range of resolution scales. Additionally, I was able to highlight key morphological predictors of each habitat metric. In utilizing Structure-from-Motion (SfM) photogrammetry, I was able to construct high-resolution three-dimensional (3D) models of reef plots across the five expeditions to extract six ecologically relevant habitat metrics and classify the reef benthos based on the morphological structure present. I found that the significant declines in the habitat structure metrics occurred before the end of the heatwave, with no further significant losses reported for the remainder of the study. Increased levels of anthropogenic disturbance compounded the effects of the marine heatwave, resulting in high disturbance sites reporting the lowest values of structural complexity throughout the study. Resolution scale altered the trends seen in the habitat metrics, with the significant yearly declines reported at 1.0 cm resolution loosing significance when coarsening to 4.0 and 8.0 cm for all habitat metrics other than planform curvature. Further justification of branching, plating, and foliose morphological growth forms as complex structures was highlighted through random forest regressions, however the inclusion of living submassive corals as a key influential morphology for the metrics of complexity was, to our knowledge, a new finding. Overall, this study is one of the first longitudinal studies investigating habitat structure throughout a mass mortality event and will further advance our understanding of reef habitat structure facing both local and global stressors.

Chapter 2 – Structural complexity change resulting from prolonged heatwave-induced mass coral mortality: Influence of underlying disturbance, model resolution, and coral morphology

Kevin Bruce[1], John Burns[2], Julia K. Baum[1]

[1] Department of Biology, University of Victoria, PO Box 1700 Station CSC, Victoria, British Columbia, V8W 2Y2, Canada

2 Marine Science Department, College of Natural and Health Sciences, University of Hawai‘i at Hilo, 200 W. Kawili Street, Hilo, Hawai‘i, 96720, USA

In preparation to be submitted as a manuscript to a peer-reviewed journal.

2.1 Abstract

Habitat structure is critically important for the maintenance of biodiversity in coral reef ecosystems. Marine heatwaves and local anthropogenic stressors threaten the persistence of reef-building coral species, and hence the structural integrity of these ecosystems. Utilizing Structure-from-Motion (SfM) photogrammetry, we quantified the immediate and long-term effects of the 2015-2016 El Niño-induced mass coral mortality event on three-dimensional (3D) reef habitat structural complexity at 30 permanent 16m^2 plots over five time points, from before (2015) to three years after (2019) the event. Sites (n=10, with 3 plots/site) were selected based on their exposure to either low, medium, or high levels of local anthropogenic disturbance. We created 3D reconstructions of each plot and examined changes in six geospatial metrics over space and time, how the spatial resolution of the digital elevation models (DEMs) influenced the habitat metrics through time, and identified the key coral morphologies creating influencing each habitat metric. Significant declines in all metrics at 1.0cm resolution, except for profile curvature range and volumetric change, occurred by the end of the heatwave (March 2016). Furthermore, we detected a net loss of habitat volume in three-quarters of the plots between 2015 and 2019, with windward sites losing more volume than sheltered ones. Increased spatial resolutions significantly altered the trends observed at 1.0cm, with yearly significance lost in most metrics by 8.0 cm resolution. Only planform curvature range retained yearly significance across all resolution scales examined. Lastly, random forest regressions explained reef complexity metrics well, pinpointing live branching, tabulate, foliose, and submassive morphologies as key morphologies influencing the complexity metrics. In the face of accelerating climate change, mitigating local stressors and furthering understanding the key elements impacting reef structure may increase reef habitat structural complexity, thereby heightening reef resilience to future thermal stress events.

2.2 Introduction

Habitat structural complexity, long associated with ecosystem productivity and organismal abundance and diversity, is created in both marine and terrestrial ecosystems by the foundation species (MacArthur and MacArthur 1961; Luckhurst and Luckhurst 1978; Steneck et al. 2002; Couch et al. 2017; Fukunaga et al. 2020a). In tropical coral reefs, habitat structural complexity (i.e. the physical three-dimensional (3D) structure of the reefscape), is primarily created by 'reef-building' (hard) Scleractinian corals (Order Scleractinia; Phylum Cnidaria) (Vaughan and Wells 1943; Bellwood et al. 2004; Graham and Nash 2013). Reef 3D structure is influenced by the surrounding environment, shaping various coral morphologies through inter- and intra-specific competition for space and light, with selection of specific morphological traits occurring in areas of environmental extremes, such as areas of high wave energy and exposure (Chappell 1980; Bradbury and Young 1981; Pratchett et al. 2015; Zawada et al. 2019; Fontoura et al. 2020). Coral morphology can be highly plastic, even within the same species (Veron 2000, 2013; Todd 2008). This plasticity creates a diverse range of habitat niches for a plethora of organisms to inhabit, thereby enabling coral reefs to be one of the most biodiverse ecosystems on the planet (Reaka-Kudla 1997; Gates and Ainsworth 2011).

The primary threat coral reefs face are climate-change amplified marine heatwaves (Eakin et al. 2016; IPCC 2019). Marine heatwaves are short-lived temperature anomalies often caused by climatic variability (eg., El Niño) altering oceanic processes that leads to increases in ocean sea surface temperature (Oliver et al. 2021) which in turn can lead to mass coral bleaching events (Eakin et al. 2016). These heatwave-induced mass bleaching events have the ability to cause significant negative impacts to reefs, by altering coral community structure (Bozec et al. 2015), increasing erosion (Sheppard et al. 2002), lowering carbonate budgets (Alvarez-Filip et al.

2013), or shifting reefs to a macroalgal dominated state (Done 1992; McManus and Polsenberg 2004). Marine heatwaves are able to be localized or global in nature, however the 2015-2016 event was felt worldwide with mass bleaching events documented worldwide (Couch et al. 2017; Hughes et al. 2017; Magel et al. 2019; Vargas-Ángel et al. 2019). Coral bleaching is a phenomenon where coral polyps physically expel the symbiotic algae, thereby giving the colony a "bleached" appearance (Glynn 1983) and may lead to mortality if the increased temperatures or ongoing stressors persist (Hoegh-Guldberg 1999). Colony susceptibility and resilience towards temperature increases has recently been linked to specific clades of the symbiotic algae (Symbiodinium spp.) located within their tissues (Glynn 1983; Heron et al. 2016; Claar et al. 2020). During these times, the coral's nutrient uptake is limited, which hinders growth through reduced accretion rates and lowers resilience to future disturbance events (Hoegh-Guldberg 1999; Hoegh-Guldberg et al. 2007; Heron et al. 2016; Couch et al. 2017). The level to which a colony bleaches may relate to the colony's morphology, as more complex coral morphologies (eg., branching) are generally more susceptible to disturbances than the slow-growing (eg., massive) morphologies (Loya et al. 2001; Gates and Ainsworth 2011). Many studies report the immediate, destructive impacts of these heatwaves (Burns et al. 2016; Couch et al. 2017; Magel et al. 2019), yet this leaves the longitudinal effects of heatwaves on habitat structure relatively unknown.

Methods to quantify reef habitat structure range from simple, in-situ measurements to broad-scale digital mapping of the reef's 3D structure. Prior to the technological advances in geomatic and photogrammetry technology, most studies examining coral reef complexity utilized either the chain-and-tape methodology (Risk 1972; Luckhurst and Luckhurst 1978) or habitat assessment scores (Wilson et al. 2007). The chain-tape method is time-consuming, labour-intensive, may cause physical damage to the live coral tissue, are at a fixed resolution scale (chain-link size), and results may vary greatly based on the placement of the chain (Knudby and LeDrew 2007; Friedman et al. 2012; Dustan et al. 2013). Habitat assessment scores are a quick qualitative method to obtain coarse reef complexity values, however visual approximations will vary based on the technician and the coarse scale may make future analyses difficult (Wilson et al. 2007; Harborne et al. 2012). Within the past decade, development of a new, user-friendly methodology called Structure-from-Motion (SfM) photogrammetry has enabled more researchers to quantify robust 3D habitat metrics of reef complexity across a multitude of resolutions, at either meso-scale (10's of square meters) and micro-scales (centimeter-millimetre) (Friedman et al. 2012; Harborne et al. 2012; Westoby et al. 2012; Figueira et al. 2015; Leon et al. 2015; Cullen et al. 2018). It is important to ensure the ecological relevance of the resolution scale examined (McCormick 1994), as resolution has been known to influence the habitat structure metric outputs from both SfM photogrammetry (Fukunaga et al. 2019a, 2020a) or in-situ chain-tape (Friedman et al. 2012) methodologies. For instance, intricate, complex coral morphologies offer fine-scale complexity and micro-habitats at fine resolutions which act as refuge space for invertebrate and juvenile fish assemblages (Hixon and Beets 1993; McCormick 1994; Wilson et al. 2010), whereas habitat metrics at meso-scale, coarser resolutions appear to more heavily impact larger fish species predation success rates (Harborne et al. 2012; Hunt et al. 2019).

Here, we employ SfM photogrammetry in a longitudinal study to examine changes in coral reef structural complexity and habitat volume over the course of a prolonged marine heatwave, and in the three years thereafter. The 2015-2016 El Niño caused a prolonged heatwave at its epicentre, Kiritimati (Republic of Kiribati) in the central equatorial Pacific, subjecting the corals to ten months of anomalous temperatures which resulted in as 89% loss of hard coral cover (Baum et al., *in prep*). The clustering of the atoll's human populous (Fig. 2.1) forms a distinct gradient of local disturbance, with sites situated towards the north-western corner of the atoll facing the highest levels of anthropogenic disturbance (Watson et al. 2016). The reef plots around the atoll utilized in this study were established by Magel et al. (2019) across a diverse array off reef conditions, ranging from pristine reefs to heavily degraded rubble barrens prior to the mass mortality event. Utilizing this 'natural experiment' framework, Structure-from-Motion photogrammetry was used during each expedition to create spatially accurate, high resolution three-dimensional (3D) models of each reef plot. These models were used to document the changes in structural complexity across both spatial and temporal scales in attempts to characterize the fluidity of structural changes occurring on reefs subject to these heat stress events. We specifically aim to *1)* quantify the change in reef structural complexity and habitat volume following a mortality event, *2)* specify to what level local anthropogenic stressors influence structural complexity and habitat volume, *3)* test if changes in model resolution alter the trends in habitat metrics values, and *4)* assess which coral morphologies contribute to different components of reef complexity.

2.3 Methods

2.3.1 Study Site and Design

Changes in 3D reef structure following the 2015-2016 El Niño induced mass coral mortality event around Kiritimati (Christmas Island, Republic of Kiribati), a remote atoll in the central equatorial Pacific Ocean (01°52′N 157°24′W, Fig. 2.1), was documented at five timepoints spanning the event: May 2015, March 2016, November 2016, July 2017, and July

2019. Sites were sampled during each expedition, however, unusually powerful weather systems during March 2016 (2016a), November 2016 (2016b), and July 2019 limited sampling (Table A.2.1) in sites located in the remote Bay of Wrecks. In 2015 our team established 16 m^2 permanent photoquadrats (PPQs) along the 10–12 m isobath at 10 sites spanning a gradient of local anthropogenic disturbance made possible by the distribution of the human population around the atoll. Each site has previously been assigned to one of three anthropogenic disturbance levels (low, medium, high) based on a combination of the intensity of fishing pressure present and proximity to local villages (Watson et al. 2016). Three PPQs were installed with approximately 10 m spacing at each study site using stainless steel stakes to demarcate the corners of each individual PPQ. The PPQs were developed to document spatial variability in benthic community composition and morphology and determine the extent to which local anthropogenic stressors influence these coral reef habitats.

2.3.2 SfM photographic surveys

Images of each PPQ were collected using accepted photogrammetry techniques for creating 3D reconstructions of coral reef habitats (Burns et al. 2015a; Leon et al. 2015; Ferrari et al. 2016; Magel et al. 2019; Bayley and Mogg 2020). Scaled ground control points (GCPs) were placed at the staked corners of each PPQ. The known depths and dimensions of the GCPs enable accurate orthorectification of the resulting 3D models. A calibration grid and scale bar were also placed along the border of the PPQ to assist with the validation of the spatial accuracy for each resulting model. Digital images of each PPQ were collected by a diver swimming in a boustrophodonic pattern approximately 1 m above the substrate. The diver collected images with 70-80% overlap from both planar and slightly oblique angles. Images were taken using a Nikon D750 digital SLR camera (Nikon Canada Inc., Mississauga, Canada) with a 24 mm Sigma lens

(Sigma Canada, Markham, Canada) and an Ikelite housing with an 8-inch hemispheric dome port (Ikelite Underwater Systems, Indianapolis, USA).

2.3.3 Three-dimensional model generation

Spatially accurate 3D reconstructions of each PPQ were rendered using the Agisoft Photoscan software (Agisoft LLC., St. Petersburg, Russia) following Burns et al. (2015a)'s detailed procedure. Camera calibration and optimization were completed using the PhotosScan software. Photoscan calibrates the imagery using Brown's distortion model to resolve optical characteristics of the lens from the image metadata (Fukunaga and Burns 2020). The photogrammetric workflow aligns the overlapping imagery and estimates camera locations for each image to produce a 3D point cloud representing the physical structure of the PPQ. The known x, y, z coordinates of the GCPs are used to create a spatially accurate local coordinate system. The software then performs self-calibrating bundle adjustments based on the GCP information to generate a dense point cloud that accurately represents the true 3D structure of the PPQ. A digital elevation model (DEM) and orthophotomosaic were generated and exported for analysis of benthic community composition and 3D structural complexity. The DEM is a 2.5D raster file containing the 3D elevation data of the reef plot within a grid of cells that can be used to quantify various metrics of architectural complexity. The orthophotomosaic is a high-resolution 2D image generated by layering and aligning the source photos. The DEM and orthophotomosaics can be aligned using the local coordinate system 3D model to enable annotation and quantitative analyses of specific benthic features (Burns et al. 2015b). 3D models, DEMs, and orthophotomosaics were rendered for the PPQs established at the 10 sites over a 5-year time space (n= 22-30 PPQ's per year).

All models rendered in Agisoft Photoscan reported ground sampling distance (GSD) values between 0.03 to 0.103 cm/pix, thus validating that the resolutions used in this study for structural analyses (1.0, 4.0, and 8.0 cm) were not outside the spatial range of model accuracy. A standard measure of spatial resolution in remote sensing, GSD is the distance between two consecutive pixel centers, with smaller values indicating 3D models possess greater spatial resolution and ability to detect intricate spatial features (Lee and Sull 2019; Fukunaga et al. 2019a; Magel et al. 2019). A DEM with cell size of 1.0 cm has been shown to effectively capture changes in the structural complexity of reef benthos (Burns et al. 2016; Couch et al. 2017), whereas both 1.0 cm and 4.0cm resolutions have been shown to relationships between reef structural complexity and coral reef fish assemblages (Fukunaga et al. 2020b). Structural complexity metrics are were computed from DEMs within 3x3 cell windows, thus our study effectively quantifies the topographic complexity of each PPQ at 3 cm, 12 cm, and 24 cm resolutions.

2.3.4 Longitudinal SfM study caveats

As this study builds on Magel et al. (2019), which compared reef structural complexity at two timepoints (before and 15 months after the end of the heatwave), we needed to expand the range of data to incorporate the five timepoints used in this study. To do so, several obstacles had to be overcome, included accurately aligning each individual PPQ across multiple timepoints, and correctly scaling the 3D models using consistent scalable objects (see Appendix C for details).

2.3.5 Metrics of 3D structural complexity

Six habitat metrics describing reef 3D structural complexity were examined in this study. Of these, three specifically examine different aspects of the reef surface's complexity (surface complexity, terrain ruggedness (VRM), fractal dimension), two explain components of reef surface curvature (profile curvature, planform curvature), and one examines reef habitat volumetric change between two timepoints (Fig A.2.6). Surface complexity is analogous to the traditional measurement of reef rugosity in that it compares the contour distance (3D) to the linear distance (2D) along either a transect or within a plot (Risk 1972; Fukunaga et al. 2019a). VRM simultaneously captures variation in both slope and aspect within a single dimensionless measurement, with values typically < 0.4 in natural data (Sappington et al. 2007; Walbridge et al. 2018). Fractal dimension (D) is a comprehensive metric describing the irregularity of an object through the comparison of the 3D surface area across different resolution scales (Mandelbrot 1982; Fukunaga and Burns 2020; Fukunaga et al. 2020a). Reported as a single value across a range of 2 to 3, increases of fractal dimension towards 3 indicate more complex environments across the resolutions examined (Kostylev et al. 2005; Young et al. 2017; Fukunaga and Burns 2020). All three of the above represent metrics describing reef surface complexity, with both fractal dimension and VRM both independent of slope, which enables them to be two of the more interpretable metrics of complexity utilized in reef habitat complexity studies (Fukunaga et al. 2020a). Overall curvature is defined as the slope of the slope and quantifies the rate of change in the reef surface, with larger values indicating more complex terrain (Pittman et al. 2009; Burns et al. 2015b). Within overall curvature are the two subcategories of profile and planform curvature, which describe the curvature of the reef structure either parallel to or perpendicular to the maximum slope (Burns et al. 2015b, 2015a). Habitat volumetric change compares the point clouds between two timepoints and calculates the change in habitat volume within that select area.

2.3.6 Ecological relevance of habitat metrics

Habitat metrics examined in this study were selected by the unique properties each describe relating to 3D structural complexity (Fukunaga and Burns 2020) and their ecological influence on both organismal abundance (Burns et al. 2015a; Leon et al. 2015; Couch et al. 2017; Fukunaga et al. 2020b) and local reef hydrodynamics (Guinan et al. 2009; Burns et al. 2011). It is important to note that these metrics are responsive to the mortality events experienced during this study, as the once live complex surfaces within the plot erode (Fukunaga and Burns 2020), with each explaining different aspects of these structural changes. As the ratio of 3D to 2D surface area within the plot, surface complexity values are indicative of potential habitat space available within the sample area, with higher values indicating more "complex" habitats which often provide more refuse space for organisms (MacArthur and MacArthur 1961; Friedlander and Parrish 1998). VRM is a measure of terrain ruggedness and is able to highlight fine-scale changes in habitat topography such a ridges, valleys, and surface roughness independent of the topography's slope, which is important as the independence of slope may alter the perception of the habitat by the organism, particularly when assessing habitat for predator avoidance measures (Sappington et al. 2007). Fractal dimension has been shown to be highly sensitive towards different morphological coral structures (Reichert et al. 2017) and in doing so, has the ability to describe how the landscape is being divided into topographically distinct microhabitats and niches for organisms to inhabit across resolution scales (Johnson et al. 2003; Kostylev et al. 2005; Torres-Pulliza et al. 2020). Both profile and planform curvature are able to report the orientation of the structure parallel (profile) and perpendicular (planform) to the maximum slope, thereby highlighting habitat such as ridges and valleys for organisms to inhabit (Pittman et al.

2009; Burns et al. 2015a). Additionally, these curvature metrics also describe hydrodynamic patters impacting food particle supply for sessile organisms (Guinan et al. 2009; Burns et al. 2011). Profile curvature describes the velocity of benthic flow while planform curvature describes the convergence or divergence of this flow on the surface (Walbridge et al. 2018). Lastly, habitat volume can have direct impacts on many local reef functions, including coral growth, carbonate production, respiration rates, and chlorophyll concentrations (Cocito et al. 2003; Lavy et al. 2015). As such, a reduction in habitat volume will affect these ecological processes, and in doing so, dimmish local reef biodiversity (Graham et al. 2006; Burns et al. 2016) and limit the ecosystem services coral reefs provide nearshore human communities (Moberg and Folke 1999).

2.3.7 Quantification of reef habitat metrics

The 3D structure of each PPQ was measured for the six metrics of structural complexity, with all but habitat volumetric change calculated using geospatial analyst tools within ArcMap (ArcGIS 10.5, Environmental Systems Resource Institute, Redlands, USA). All habitat metrics were initially quantified with the DEM cell size set to 1.0cm, as this resolution scale has been effective in past studies capturing structural complexity changes on coral reefs (Burns et al. 2016; Ferrari et al. 2016, 2017; Couch et al. 2017; Magel et al. 2019). The "Pre-heatwave" 2015 PPQs were used as the baseline to measure changes occurring across the temporal gradient of this study. The DEMs and orthophotomosaics were exported in consistent alignment and orientation for each year to accurately measure changes in habitat structural complexity through time. Surface complexity was calculated as the ratio of 3D surface area to 2D surface area within the PPQ polygon (Fukunaga et al. 2019a). VRM, profile curvature, and planform curvature were computed from the surface properties of the DEM raster's cells within a 3X3 window, with the mean value of VRM noted and the ranges of both curvature metrics calculated from the maximum and minimum values present within the PPQ area. As reporting the average curvature value may be an oversimplification for a non-static metric, we instead calculated the range of each curvature metric within the PPQ, which has been shown to be far more telling of the topographic landscape present (Young et al. 2017; Fukunaga et al. 2019a). Fractal dimension was calculated using the equation $F_D = 2 - \text{slope}[\log S(s)/\log(s)]$, where s is the resolution of the DEM set in meters (eg., 0.01, 0.04, or 0.08) and S(s) is the 3D surface area of the plot at a given resolution.

As the values computed for structural complexity metrics are influenced by the raster cell resolution used to examine them (Knudby and LeDrew 2007; Friedman et al. 2012; Burns et al. 2015a; Fukunaga et al. 2020a), we additionally quantified each geospatial habitat metric at three cell resolutions (1, 4, and 8cm) known to respond to changes in live coral cover and composition (Leon et al. 2015; Couch et al. 2017; Fukunaga et al. 2019b, 2020a). However, of the geospatial metrics used in this study, only surface complexity, VRM, profile curvature range and, planform curvature range were able to be quantified at the additional resolutions as neither fractal dimension nor volumetric change can be quantified at multiple resolutions. Fractal dimension is a metric that examines 3D surface area present across a range of resolution scales (Young et al. 2017; Fukunaga et al. 2019a) while habitat volumetric change is derived from point cloud data which is set to the lowest possible resolution.

Habitat volumetric change was calculated using the open-source software CloudCompare (Version 2.10.2) (Fig A.2.2). Point clouds rendered during the 3D reconstruction process can be aligned using the fixed pins of the PPQs. Once aligned, the software is capable of quantifying positive and negative changes in volumetric properties between the two time points (Fig. A.2.2, Fig A.2.6). This process produces a singular value of volumetric habitat change for each comparison of two time points. Point clouds representing the PPQ's from 2015, 2017, and 2019 were compared in pair-wise combinations following methods used to document temporal changes in the volume of reef habitats (Burns et al. 2016; Magel et al. 2019; Bayley and Mogg 2020). Point clouds were initially aligned by performing a rough alignment using the PPQ plot boundary pins as reference points. Fine registration was then conducted using the Iterative Closet Point (ICP) algorithm to allow for adjusting the scaling of the source point cloud to the reference point cloud. After alignment is completed, the 2.5D volume computation tool computes the precise volumetric difference between the point clouds. For this study, PPQ point clouds volumetric change was broken down into three distinct time intervals: 1) 2015- 2017, which acts as the change between volume prior to the heatwave and up to 15 months after the heatwave ended, 2) 2017-2019, which computes the changes in volume from 15 months to nearly 3 years post heatwave, and 3) 2015-2019, which reports net volumetric change throughout the entire study. By breaking down the study into these distinct time intervals, we can determine whether the change in habitat volume across the years was continual or more of a "pulse" degradation.

2.3.8 Analysis of Benthic Morphology Composition

The high resolution orthophotomosaics of the PPQ's from 2015, 2017, and 2019 were used to characterize benthic community composition. Individual corals were annotated based on their morphological attributes using an identification schema designed from past morphological studies specifically for the coral taxa found around Kiritimati (English and Wilkinson 1994; Edinger and Risk 2000; Pratchett et al. 2015). All live coral colonies in each PPQ were digitally annotated by experienced technicians trained in coral identification using ArcGIS editor tools. A "feature class" layer was created with the morphological identification template listed as individual sub-groups within the feature class. Each plot required 6 hours on average to fully annotate, amounting to 240 total hours to complete full semantic segmentation of the PPQs.

2.3.9 Statistical Analyses

All statistical analyses were conducted in R version 4.0.3 (R Core Team 2019) to fit linear mixed-effect models using the package "lme4" to quantify the influences of local and global stressors on each of the habitat metrics sampled: surface complexity, VRM, fractal dimension, profile curvature range, planform curvature range, and habitat volumetric change. For each metric, models were fit with expedition year, site exposure, and anthropogenic disturbance as fixed-effects and site as a random effect to account for PPQ non-independence (Magel et al. 2019). We modelled local anthropogenic disturbance as a continuous variable and both site exposure (i.e., leeward vs. windward) and expedition year as categorical variables. We evaluated 13 models for each habitat metric by fitting every combination of covariates listed above, including an interaction term between expedition year and local anthropogenic disturbance. AICc was used to compare models and select a best-fit model set within Δ4 AICc using model selection and multi-model inference (Burnham and Anderson 2004) . Model normality and homogeneity of variance were evaluated graphically for all models retained in the top model set and all appeared to be reasonable fits. We acknowledge that metrics for the years following the heatwave may have been temporally autocorrelated, however I did not explicitly test for this. Following model selection, post-hoc analyses on expedition year were conducted for each habitat metric on the raw data at 1.0cm resolution (Fig. 2.2) using *emmeans* (Lenth 2017). We later computed the top model's predicted values across the local anthropogenic disturbance gradient for each habitat metric (Fig. 2.3) using ggplot2 (Wickham 2016).

To determine morphologies associated with temporal fluctuations in live coral cover, random forest regressions (RFs) were applied using the *randomForest* package (Liaw and Wiener 2002). RFs are a user-friendly machine-learning analysis where multiple sets of decision trees are constructed using a different bootstrapped sample of the data for each tree to determine top predictors of the response variable within the dataset (Brieman 2001; Liaw and Wiener 2002; Fox et al. 2017). An effective predictive tool that prevents overfitting through randomly bootstrapping the dataset, RFs are able to compute the level of variance explained by the predictor variables and each variable's importance to the model (Brieman 2001; Prasad et al. 2006; Cutler et al. 2007; Fox et al. 2017). The RF algorithm splits data into training (66%) and test (33%) datasets and train themselves on the larger dataset before running model validation on the remaining un-trained dataset to provide the variance explained, mean of square residuals of the model, and variable importance measures (Liaw and Wiener 2002; Prasad et al. 2006). Random forests are able to be fine-tuned by the altering of two parameters within the model (number of trees in the forest and number of variables at each tree branch), however literature is mixed whether tuning these variables make any significant difference (Brieman 2001; Liaw and Wiener 2002; Strobl et al. 2008; Fox et al. 2017). Two qualitative measures of variable importance describing the predictive power of the analysis are computed during RF's. Increased Mean Square Error (%IncMSE) accounts for the mean decrease in accuracy when a variable's value is changed or permuted, with higher %IncMSE signifying higher variable important, and Increased Impurity Index (IncNodePurity), which relates to the loss of function at each branch (node) of the regression tree if the predictor is removed, with more useful variables reporting higher increases in node purities (Echeverry-Galvis et al. 2014; Dewi and Chen). This resulted with the compilation of a top-5 coral morphologies dominating the PPQ for each metric of habitat complexity and curvature described in Table 2.2.

2.4 Results

2.4.1 Habitat structural degradation over time

All habitat metrics of complexity and curvature were significantly influenced by expedition year, local disturbance, and site exposure at the 1.0 cm resolution (Table 2.1). All metrics of complexity and planform curvature declined during the prolonged heatwave, with each significantly lower by the end of the heatwave (March/April 2016) than before it (May 2015) (Fig. 2.2). However, none of these metrics declined significantly thereafter, such that the two subsequent two time points (i.e., November 2016 (seven months after the heatwave) or July 2017 (15 months after the heatwave) were not significantly different than at the end of heatwave time (Fig. 2.2, Table 2.1). By three years after the end of the heatwave (2019), all metrics of habitat complexity and planform curvature showed significant increases from 2017. In addition to these temporal changes, all metrics were negatively related to chronic local anthropogenic disturbance (Table 2.1). Testing the two-way interaction between year and local disturbance, we found that it was only significant for VRM, such that the slope of this negative relationship was significantly shallower in 2017 than 2015 (Fig. 2.3). Site exposure was statistically significant for all complexity metrics and for profile curvature range, with exposed sites (i.e., windward) having significantly higher values of complexity and curvature (Table 2.1).

Net loss of reef habitat volume occurred from before (2015) to three years after (2019) the heatwave at 16 of 21 total PPQs (6 of 7 sites sampled in both 2015 and 2019; range of change: -1.97m^3 to + 0.513m^3). Comparing habitat volumetric change for the periods 2015 to 2017 and 2015 to 2019, it is evident that reef volume did not degrade linearly over time (Fig 2.2). Habitat volumetric loss was greater from 2015 to 2017 (-1.365m^3 to +0.419m^3) than in the subsequent two years (-0.883m^3 to +0.641m^3). While volumetric change was not significantly different between the 2015-2017 and 2017-2019 time intervals, 81% of the plots (21 of 26) experienced a loss of habitat volume between 2015 and 2017, whereas only 42% of plots (10 of 24) experienced loss between 2017 and 2019. Additionally, habitat volume was influenced significantly by site exposure, with windward sites experiencing significantly larger declines than leeward ones. Local anthropogenic disturbance was not selected as a key predictor in the best fit model (Table 2.1).

2.4.2 Influence of spatial resolution on perceptions of structural complexity

The relationship between the metrics of habitat complexity and curvature and expedition year differed depending on the resolution of the 3D model used to compute them. Planform curvature range was the only metric to retain yearly significance across all three resolutions examined, while other habitat metrics lost yearly significance at either 8.0cm (VRM), 4.0cm (surface complexity), or never reported yearly significance (profile curvature range) respectively (Fig. 2.4; Table A.2.2). Site exposure and local disturbance both proved significant across all resolutions whenever included in the top model fit.

2.4.3 Key morphological components of structural complexity

Random forest regression results differed between the habitat metrics sampled, with metrics of complexity (surface complexity, VRM, and fractal dimension) far outperforming metrics of curvature (profile and planform curvature ranges) (Table 2.2). The impact of morphological structure on habitat volumetric loss was not examined as we were more interested in answering whether live or dead structure was influencing the geospatial habitat metrics across the years. Results across different model tunings were broadly similar, with the complex morphology of the full collection of live and abiotic structure using default RF settings generally best explaining the metrics (Table B.2.1). Exclusion of abiotic structure made very little difference in variance explained, with only VRM showing an improvement. See appendix B for full comparisons between the different tunable parameters, simple vs complex classification systems, and abiotic vs full datasets. Overall, the complex classification system (including abiotic structure, default tuning settings) explained 49.9 – 53.4% of the variation amongst the habitat complexity metrics (Table 2.2). Live submassive, branching, and foliose morphologies were key predictors for all complexity metrics, with live tabulate important for VRM and surface complexity (Table 2.2, Fig. 2.6). Fractal dimension included these live morphologies in its top predictors along with multiple abiotic structures (dead branching and dead tabulate). In contrast, RFs only explained between 9.8 – 10.4% of the variance within either curvature metric (Table 2.2), indicating that this method of determining key morphological influencers for curvature range wasn't particularly insightful. Of the listed morphologies, live foliose was a notable absence from the top predictors of curvature compared to that of the complexity metrics. Instead, "less complex" morphologies were selected as top predictors such as live massive, encrusting, and *Porites*.

2.5 Discussion

This study, which to our knowledge includes the most time points examining coral reef structural change arising from a mass mortality event, reveals several new facets of the degradation of habitat structural complexity. First, the degradation of habitat structure can occur quickly following coral mortality. Contrary to our predictions, the most significant structural loss in all habitat metrics of complexity occurred by the end of the heatwave in March 2016. Habitat volume did not report significant differences in volumetric change between the two separate time intervals tested, however site exposure proved significant as sites experiencing windward exposure reported greater declines in habitat volume. Second, resolution scale significantly impacted the habitat metrics trends as we predicted, with the yearly significance noted at the 1.0cm scale lost as resolution coarsened for all metrics other than planform curvature range. Third, local anthropogenic disturbance was found to negatively impact the habitat metrics across all three ecological scales reported in this study. Finally, live branching, tabulate, foliose, and submassive morphologies were all selected as top predictors contributing towards reef structural complexity. The inclusion of the submassive morphology was surprising, as this morphology hasn't been stated as a source of complexity in any prior morphological studies.

2.5.1 Structural Complexity Degradation Through Time.

Changes to 3D structural complexity throughout a disturbance event are becoming more well documented in the scientific literature the past decade (Alvarez-Filip et al. 2009; Graham and Nash 2013; Bozec et al. 2015; Burns et al. 2016). Generally, our result of structural decline following disturbance corroborate findings from similar SfM studies (Burns et al. 2016; Couch et al. 2017; Magel et al. 2019), however the rapid nature in which significant declines occurred while the heatwave was ongoing is, to our knowledge, a first. We speculate that increased wave energy during the winter months separating our first two expeditions (May 2015 and March 2016) caused mass fragmentation of the recently deceased, structurally vulnerable, "complex" coral colonies. As these morphologies are often disproportionately impacted by these heatwaves (Loya et al. 2001; Couch et al. 2017), we hypothesize the mortality and subsequent fragmentation of the complex morphological species dominant around Kiritimati (eg. *Acropora* spp., *Montipora* spp.) was the catalyst to the declines in structural complexity reported. This hypothesis was validated by the random forest regression results as these complex morphologies were highlighted as top influencers of habitat complexity for terrain ruggedness (VRM), surface complexity, and fractal dimension. This destruction of the complex coral morphologies was visually evident in the time-series photographs of the plots (Fig. 2.5) and through the habitat volumetric analysis, whereby multiple plots experienced more than $1m^3$ of volumetric loss throughout the study, with larger declines reported in the initial 2015-2017 time interval (Fig. 2.2). Despite this loss in habitat volume throughout the study, the habitat metrics of structural complexity showed no further declines following the initial significant decrease, indicating that at fine resolutions, these geospatial metrics do not effectively capture changes in habitat volume.

The fragmentation of the complex coral morphologies effectively altered the coral community structure around Kiritimati, shifting site communities towards less-complex, massive and submassive dominated structure. The inclusion of live submassive and *Porites* morphological structures as key predictors in habitat structural complexity was unexpected, as neither of these have previously been highlighted as being structurally complex. With that said, many of the submassive colonies have irregular ridges or lumps across their surfaces, which would influence the habitat metrics at the fine 1.0cm resolution scale reported in this study. To further complicate matters, many of the submassive colonies died during the heatwave, despite having a supposed higher tolerance towards environmental stressors (Loya et al. 2001; Claar et al. 2020), which left them open to erosion and fragmentation. However, these morphologies often have higher surface areas securely attached to the reef matrix which allows them to be less prone to mass fragmentation and experience the subsequent declines in habitat structural complexity seen with branching, plating, and foliose morphologies (Torda et al. 2018). As *Porites* is known for its heat tolerance (Hoegh-Guldberg and Salvat 1995; Loya et al. 2001) and was one of the few species around Kiritimati to survive the heatwave in high numbers (Claar and Baum 2019), its inclusion as a top predictor is hypothesized to be due to its consistent presence across all sites and years rather than being a true driver of complexity. It is important to point out the difference highlighted through the RF regressions between massive, submassive, and *Porites* mounding-lobate structure's contributions towards reef habitat structure. This delineation between the massive morphology and the submassive and *Porites* morphologies highlights that coarse classification of coral morphology may hide the subtle differences between structure types and that refined morphological analyses of the relationship between coral colony morphology and habitat structure could highlight new trends in the field.

Following the initial significant declines, the habitat metrics remained significantly unchanged for the remainder of the study, which could indicate the lowest level of 3D structural complexity for these reef habitats was reached. However, it is naïve to believe that erosion and further degradation of the PPQ's ceased to continue following the mass declines experienced by March 2016. Instead, we believe that this minimal change in reef structure up until 2019 was a result of the natural erosional forces being offset by a combination of a large bloom of fleshy macroalgae, surviving coral's growth over that period, and rubble transport into, and subsequent fragmentation within, the PPQ. Following the mass coral mortality, many sites experienced a short-lived bloom of fleshy macroalgae that we hypothesize added to both habitat volume and fine-scale complexity to various extents (Fig. A.2.3). Surviving coral's continued growth was evident when examining the plots through time (Fig 2.5) and is believed to have further offset the constant erosion. Additionally, rubble transport from wave energy appears to have both brought new rubble into many plots and further fragmented the pieces present, thereby creating more fine scale "ridges" and "valleys" within the rubble fields. This rubble transport was particularly evident in the high disturbance sites (Fig. A.2.4). This observation leads us to believe that we are documenting habitat metric's response to the dynamics of rubble transport rather than changes coral reef structural complexity.

All habitat metrics except profile curvature range significantly increased between 2017 and 2019, potentially indicating the regeneration of the reef's 3D structure following the mass mortality event. However, as these significant increases only occurred at the 1.0cm resolution scale, we hypothesize that is not solely indicating regeneration. Instead, we believe these increases are due to a combination of continued coral growth from the colonies that survived the heatwave, recruitment of new juvenile coral species (particularly the branching *Pocillopora* spp. corals observed in many sites in 2019), and further erosion of the remaining massive abiotic structure. This continued erosion creates fault lines and fractures to appear in those structures, which are captured by the complexity metrics as added terrain "roughness".

2.5.2 The importance of scale resolution

We found evidence that the trends of temporal structural change are influenced by the spatial resolution of the 3D model used to examine them. Specifically, we found that as the resolution scale coarsened, the declines noted between May 2015 and March 2016 lost their significance in all metrics of complexity and profile curvature range. This is not entirely unexpected, as coarsening the resolution scale effectively makes the pixels examining the plot larger (DeJong and Burrough 1995), which will blur the fine-scale ridges and valleys created by the complex coral morphologies. Most Structure-from-Motion studies to date have used a resolution of 1.0cm (Burns et al. 2016; Storlazzi et al. 2016), with a few studies examining the impact of resolution scale on coral reef structural complexity through simulated morphological structures (Fukunaga and Burns 2020) and in-situ living coral structure (Fukunaga et al. 2020a). With the knowledge that resolution scale impacts the conclusions of the study, the question needs to be asked: What resolution is most ecologically appropriate to use when reporting coral reef structural complexity? This is a question yet to be fully answered, and we believe will depend on the ultimate goals of the study examining them. If the aim is to relate the metrics of reef habitat structure to habitat availability for fishes, a resolution scale of an appropriate size for the fish study subjects would be required (Harborne et al. 2012). Instead, if the goal is to connect reef habitat structure to the presence of reef fish populations, it has been shown that fine-scale resolutions of habitat complexity and curvature impact these assemblages, as these values effectively capture the fine-scale alterations of the polyps of the coral colonies many fish rely upon as a primary food source (Fukunaga et al. 2020b). Larger resolutions may be more applicable when examining predator-prey interactions (Hunt et al. 2019), with a multi-resolution approach useful for reef monitoring programs (Fukunaga et al. 2019a).

2.5.3 Impacts of anthropogenic disturbance on coral reefs

This study illustrates the negative impacts local anthropogenic disturbance can have on coral reef 3D structural complexity across multiple ecological scales. Our findings illustrate that higher levels of anthropogenic stressors lower habitat structural complexity and effectively compounds the effects of global climate events which work additively to limit reef habitat structural complexity increases. Furthermore, these high levels of disturbance limit coral recolonization to the area as mobile rubble provide poor recruitment locations for juvenile corals (Chong-Seng et al. 2014), which essentially limits the ability of the reef matrix to grow or replenish itself via coral accretion and opens the area up to further structural fragmentation. Therefore, these high levels of disturbance compounded with the effects of the marine heatwave have caused these sites to transform into rubble-dominated sites to points where future reef recolonization of the area seem unlikely.

Sites located along the leeward side of the atoll south of the lagoon mouth experienced moderate levels of anthropogenic disturbance throughout the study. While experiencing similar metric declines of complexity and curvature, these sites experienced minimal habitat volumetric loss throughout the study. This seemed odd and we believe that the cause of this began in January 2015, when a stronger than normal tropical storm hit these sites, causing observable physical damage to the complex branching and foliose structures present (Tietjen KL, *pers. obs.*). Therefore, we hypothesize that the lack of volumetric decline at those sites is due to majority of the complex coral structure being partially fragmented or destroyed 6 months prior to our initial baseline assessment in 2015, whereas we documented the death and subsequent loss of these structures at the sites in the other levels of disturbance. If we expand further on this hypothesis, we believe that this lack of more complex corals present during that initial expedition may have lowered the baseline habitat structure values to levels lower than normal, which may cause future values to exceed our "baseline" year far sooner than at the other levels of anthropogenic disturbance.

Site exposure to hypothesized increased levels of wave energy proved to endure significantly larger habitat volumetric loss throughout the study. However, it is worth noting that this covariate is essentially layered within the local anthropogenic disturbance gradient and as such, is best used to compare structural changes between the sites experiencing low anthropogenic disturbance, as those sites are evenly split between the leeward Vaskess Bay and the windward Bay of Wrecks. Prior to the heatwave, the Bay of Wrecks sites were dominated by the presence of mature coral communities of tabulate and foliose morphologies, whereas Vaskess Bay was comprised of more massive, branching, and soft coral morphologies. Following the mass mortality event, the Bay of Wrecks experienced larger losses of complexity compared to Vaskess bay and had more visual fragmentation of the structure (Fig. A.2.5). This combination of fragile, recently deceased morphologies and higher site exposure to winter storm energy are hypothesized to have caused the mass fragmentation of these complex morphological structures present in the Bay of Wrecks.

2.5.4 Future Direction

To our knowledge, this is the first study utilizing the novel SfM photogrammetry approach to track longitudinal changes in reef 3D structural complexity at permanent plots at multiple timepoints. Past studies attempting a similar feat often rely on two comparison timepoints before and after a disturbance event (Magel et al. 2019) or use haphazardly thrown plots along a transect as proxies of reef structural complexity at that given timepoint (Burns et al.

2016; Couch et al. 2017). This ability to directly compare changes in permanent reef survey plots through time has provided our study with comparable plots through time, which allows for hypotheses to form from visual observation on coral taxa's resilience, or lack thereof, to heat stress (Fig. 2.5). For this particular study, linking metrics of habitat complexity to the reef fish assemblages is the next logical progression for this field, similar to how Fukunaga et al. (2020b) found clear trends in the relationships between certain fish functional groups and reef habitat metrics, particularly at 1.0 and 4.0cm resolution scales. We believe that the fine-scale complexity changes that occurred around Kiritimati could have negatively impacted the fish assemblages present, particularly the corallivorous fish populations that rely upon living coral as primary food sources (Graham et al. 2009). Lastly, we firmly believe further studies examining reef structural complexity's response to marine heatwave conditions should be conducted using SfM photogrammetry versus in-situ measurements due to SfM's ability to store lasting orthorectified models of reefs. As SfM photogrammetry provides a "snapshot" of the reef at that moment in time, it enables researchers to publish their results immediately with the ability to return to these plots in the future for re-analysis if new novel habitat metrics are conceived.

2.5.5 Conclusion

With future projections indicating marine heatwaves and anthropogenic stressors will continue to negatively impact coral reefs in the future (IPCC 2019), it is imperative that we further elucidate the relationship between coral reef habitat structural complexity and these stressors. One of the first longitudinal SfM studies examining this relationship, our study illustrates how significant declines in all habitat structure metrics around Kiritimati occurred during the heatwave yet did not significantly change thereafter. The effect of varying levels of local anthropogenic disturbance was significant across all resolution scales examined, with sites facing higher anthropogenic disturbance reporting lower values of structural complexity. These findings add to past Kiritimati research examining impacts of both local anthropogenic and global marine heatwave stressors on coral survival (Claar et al. 2020), coral symbioses (McDevitt-Irwin et al. 2019), and fish assemblages (Magel et al. 2020) while further indicating the need to limit these stressors on reefs moving forward into the Anthropocene. With climate change progressing rapidly and millions of people worldwide relying on reefs for sustenance, shoreline protection, and as their main method of income (Moberg and Folke 1999; Spalding et al. 2017), it has never been more crucial to find a solution managing the effect of these stressors to these ecosystems. This management needs to evolve into a universal approach tackling both the local and global stressors facing coral reefs. This can be achieved through a combination of improving local education and awareness towards mitigating local anthropogenic disturbance on reefs while simultaneously working to drastically reduce greenhouse gas emissions, fund alternative energy initiatives, and work with both local and international governing agencies to manage the impacts on coral reefs worldwide to preserve the biodiversity left in these “rainforests of the sea”.

Chapter 3 - Conclusion

Global climate change and associated marine heatwaves pose significant threats to the future of coral reefs (IPCC 2019; Oliver et al. 2021) As the destructive properties of these marine heatwaves weren't fully realized until this past decade, few studies have examined the long-term impacts these heatwaves pose to coral reef structure. This study aims to fill this knowledge gap by providing what we believe to be the first longitudinal study examining the impacts a marine heatwave-induced mass mortality event had on coral reef structural complexity. As episodes of extreme heat stress and subsequent coral bleaching are projected to become more frequent and severe in the future (Hughes et al. 2018a; IPCC 2019), determining methods to help conserve the reef structure will become even more critical. Therefore, further understanding of the relationship between coral reef structural complexity and marine heatwaves is vital.

In Chapter two, we conducted one of the first longitudinal studies examine reef structural complexity utilizing Structure-from-Motion (SfM) photogrammetry. In doing so, reef structural complexity was characterized within permanent photoquadrats (PPQs) at 10 forereef sites across a gradient of local anthropogenic disturbance around Kiritimati (Republic of Kiribati) over a four-year period. During the study we elucidate the changes in six ecologically relevant habitat metrics used in past studies to describe reef structural complexity, examine the impacts resolution scale has on the habitat metric conclusions, and determine key structural morphologies associated with the temporal fluctuations of live coral. We found that significant declines in many of the habitat metrics occurred by the end of the heatwave, with no further significant declines occurring thereafter (Fig. 2.2). Additionally, the significance between years was lost when the resolution scale was increased from 1.0cm to 4.0 and later 8.0cm for all metrics of complexity and profile curvature range (Fig. 2.4), indicating the declines were most likely capturing the fine scale changes in reef complexity as the reefscape transformed from a live-coral dominated state to one dominated by abiotic structure throughout the heatwave. Moreover, we found that anthropogenic disturbance negatively impacts reef structural complexity across all resolution scales examined, resulting in the highest values of structural complexity being found at sites with the lowest levels of local anthropogenic disturbance (Fig A.2.1). Habitat volumetric change failed to include local anthropogenic disturbance in the best fit model, but site exposure was found to be significantly impacted by the site exposure to hypothetical wave energy rather than local anthropogenic, with windward reefs experiencing significantly larger habitat volumetric declines. It is important to note however that the windward site exposure classification contains only two sites, both of which are classified as low anthropogenic disturbance (Fig 2.1), indicating site exposure to wave energy compounded the impacts of the local anthropogenic disturbance and the mass mortality event on reef structural complexity. Lastly, historically complex live branching, tabulate, and foliose morphological growth forms were highlighted as being key influencers in multiple habitat metrics (Table 2.2), with live submassive also included in many top predictor sets, which is a believed to be the first time this morphology has been pinpointed as being structurally complex. In sum, these results further highlight the negative impacts both local and global stressors have on coral reef structural complexity and volume, while showing the need to further expand the field of reef structure research within marine ecology labs to potentially assist with future efforts to reduce the severe impacts future marine heatwaves are projected to have on reef ecosystems.

Potential future studies utilizing an SfM framework are numerous and would be relatively easy to incorporate around Kiritimati. As current limitations within the experimental design limited this study to specific depth constraints (10-12m isobaths), a logical progression could be to examine structural complexity and key influencing structural morphologies as depth changes. Additionally, SfM transects data could be combined with fish census data to examine fish assemblage relationships to various aspects of coral reef structural complexity. This could include examining the simple relationships between fish functional groups and various habitat metrics, determining ecologically relevant resolution scales to examine the different fish assemblage groups, or investigating single fish specie's relationship with different morphological structures. Additionally, this current study could be broadened to further develop baseline data on further habitat metrics on coral reef habitat structural complexity not used in this study and could prove to be particularly beneficial if attempting to link ecological functions of fishes or invertebrates to different aspects of structure, possibly through metrics such as viewshed analysis (Oakley-Cogan et al. 2020), habitat convexity (Fontoura et al. 2020), and grazing surface area (González-Rivero et al. 2017). Furthermore, as this was one of the first longitudinal studies to examine reef structure throughout a mass mortality event, the obstacles (see Appendix C) that required resolving prior to completing the habitat metric quantification could be examined further to improve methods of securing plot corner stakes within the reefscape suitable for longitudinal studies and to develop ways to speed up the process of quantifying the habit metrics, similar to how Fukunaga et al. (2019) automated this process within R.

In sum, this study illustrates the rapid nature that fine-scale coral reef structural declines can occur during marine heatwaves and across levels of local anthropogenic disturbance, while highlighting the importance of resolution scale and presence of key morphological structures important in promoting high reef structural complexity. Overall, these findings illustrate the negative impact the 2015-2016 El Niño mass mortality event had on reef structural complexity around Kiritimati and highlights the need to find ways to mitigate these heatwaves from occurring in the future. This is particularly urgent as the significant declines in structural complexity were noted by the end of the heatwave, indicating high levels of structural complexity are tied to the presence of live, morphologically complex coral colonies. It is our hope that this study helps pave the way for additional longitudinal SfM studies examining reef structure, as we believe SfM photogrammetry provides a non-invasive, cost-effective, and accurate monitoring system that would be a perfect addition to marine ecological research worldwide.

Bibliography

Agudo-Adriani EA, Cappelletto J, Cavada-Blanco F, Cróquer A (2019) Structural Complexity and Benthic Cover Explain Reef-Scale Variability of Fish Assemblages in Los Roques National Park, Venezuela. Front Mar Sci 6:690

Alvarez-Filip L, Carricart-Ganivet JP, Horta-Puga G, Iglesias-Prieto R (2013) Shifts in coral-assemblage composition do not ensure persistence of reef functionality. Sci Rep 3:3486

Alvarez-Filip L, Dulvy NK, Gill JA, Côté IM, Watkinson AR (2009) Flattening of Caribbean coral reefs: region-wide declines in architectural complexity. Proc R Soc B Biol Sci 276:3019–3025

Alvarez-Filip L, Paddack MJ, Collen B, Robertson DR, Côté IM (2015) Simplification of Caribbean Reef-Fish Assemblages over Decades of Coral Reef Degradation. PLOS ONE 10:e0126004

August PV (1983) The Role of Habitat Complexity and Heterogeneity in Structuring Tropical Mammal Communities. Ecology 64:1495–1507

Baird A, Álvarez-Noriega M, Cumbo V, Connolly S, Dornelas M, Madin J (2018) Effects of tropical storms on the demography of reef corals. Mar Ecol Prog Ser 606:29–38

Bayley DTI, Mogg AOM (2020) A protocol for the large-scale analysis of reefs using Structure from Motion photogrammetry. Methods Ecol Evol 11:1410–1420

Bellwood DR, Choat JH (1990) A functional analysis of grazing in parrotfishes (family Scaridae): the ecological implications. Environ Biol Fishes 28:189–214

Bellwood DR, Hughes TP, Folke C, Nyström M (2004) Confronting the coral reef crisis. Nature 429:827–833

Boström-Einarsson L, Babcock RC, Bayraktarov E, Ceccarelli D, Cook N, Ferse SCA, Hancock B, Harrison P, Hein M, Shaver E, Smith A, Suggett D, Stewart-Sinclair PJ, Vardi T, McLeod IM (2020) Coral restoration – A systematic review of current methods, successes, failures and future directions. PLOS ONE 15:e0226631

Bozec Y-M, Alvarez-Filip L, Mumby PJ (2015) The dynamics of architectural complexity on coral reefs under climate change. Glob Change Biol 21:223–235

Bradbury R, Young P (1981) The Effects of a Major Forcing Function, Wave Energy, on a Coral Reef Ecosystem. Mar Ecol Prog Ser 5:229–241

Brieman L (2001) Random Forests. Mach Learn 45:5–32

van den Brink PJ, Mann RM, Negri AP, Uthicke S, F. Mueller J (2011) Chemical Pollution on Coral Reefs: Exposure and Ecological Effects. Ecol Impacts Toxic Chem Open Access 187–211

Brown BE (1997) Coral bleaching: Causes and consequences. Coral Reefs 16:129–138

Burnham KP, Anderson DR (2004) Multimodel Inference: Understanding AIC and BIC in Model Selection. Sociol Methods Res 33:261–304

Burns J, Delparte D, Gates R, Takabayashi M (2015a) Integrating structure-from-motion photogrammetry with geospatial software as a novel technique for quantifying 3D ecological characteristics of coral reefs. PeerJ 3:e1077

Burns JHR, Delparte D, Gates RD, Takabayashi M (2015b) Utilizing underwater three-dimensional modeling to enhance ecological and biological studies of coral reefs. ISPRS - Int Arch Photogramm Remote Sens Spat Inf Sci XL-5/W5:61–66

Burns JHR, Delparte D, Kapono L, Belt M, Gates RD, Takabayashi M (2016) Assessing the impact of acute disturbances on the structure and composition of a coral community using innovative 3D reconstruction techniques. Methods Oceanogr 15–16:49–59

Burns JHR, Rozet NK, Takabayashi M (2011) Morphology, severity, and distribution of growth anomalies in the coral, Montipora capitata, at Waiʻōpae, Hawaiʻi. Coral Reefs 30:819–826

Ceccarelli DM, McLeod IM, Boström-Einarsson L, Bryan SE, Chartrand KM, Emslie MJ, Gibbs MT, Gonzalez Rivero M, Hein MY, Heyward A, Kenyon TM, Lewis BM, Mattocks N, Newlands M, Schläppy M-L, Suggett DJ, Bay LK (2020) Substrate stabilisation and small structures in coral restoration: State of knowledge, and considerations for management and implementation. PLOS ONE 15:e0240846

Chappell J (1980) Coral morphology, diversity and reef growth. Nature 286:249–252

Chong-Seng KM, Graham NAJ, Pratchett MS (2014) Bottlenecks to coral recovery in the Seychelles. Coral Reefs 33:449–461

Claar DC, Baum JK (2019) Timing matters: survey timing during extended heat stress can influence perceptions of coral susceptibility to bleaching. Coral Reefs 38:559–565

Claar DC, Starko S, Tietjen KL, Epstein HE, Cunning R, Cobb KM, Baker AC, Gates RD, Baum JK (2020) Dynamic symbioses reveal pathways to coral survival through prolonged heatwaves. Nat Commun 11:6097

Claar DC, Szostek L, McDevitt-Irwin JM, Schanze JJ, Baum JK (2018) Global patterns and impacts of El Niño events on coral reefs: A meta-analysis. PLOS ONE 13:e0190957

Cocito S, Sgorbini S, Peirano A, Valle M (2003) 3-D reconstruction of biological objects using underwater video technique and image processing. J Exp Mar Biol Ecol 297:57–70

Cole AJ, Pratchett MS, Jones GP (2008) Diversity and functional importance of coral-feeding fishes on tropical coral reefs. Fish Fish 9:286–307

Costa BM, Battista TA, Pittman SJ (2009) Comparative evaluation of airborne LiDAR and ship-based multibeam SoNAR bathymetry and intensity for mapping coral reef ecosystems. Remote Sens Environ 113:1082–1100

Couch CS, Burns JHR, Liu G, Steward K, Gutlay TN, Kenyon J, Eakin CM, Kosaki RK (2017) Mass coral bleaching due to unprecedented marine heatwave in Papahānaumokuākea Marine National Monument (Northwestern Hawaiian Islands). PLOS ONE 12:e0185121

Cullen ND, Verma AK, Bourke MC (2018) A comparison of structure from motion photogrammetry and the traversing micro-erosion meter for measuring erosion on shore platforms. Earth Surf Dyn 6:1023–1039

Cutler DR, Edwards TC, Beard KH, Cutler A, Hess KT, Gibson J, Lawler JJ (2007) Random forests for classification in ecology. Ecology 88:2783–2792

van Dam JW, Negri AP, Uthicke S, Mueller JF (2011) Chemical Pollution on Coral Reefs: Exposure and Ecological Effects. 25

Darling ES, Graham NAJ, Januchowski-Hartley FA, Nash KL, Pratchett MS, Wilson SK (2017) Relationships between structural complexity, coral traits, and reef fish assemblages. Coral Reefs 36:561–575

Dayton PK (1985) Dayton (1983) Ecology of Kelp Communities.pdf. Annu Rev Ecol Syst 16:215–245

DeJong S, Burrough P (1995) A fractal approach to the classification of Mediterranean vegetation types in remotely sensed images. Photogramm Eng Remote Sens 1041–1053

Delparte DM, Belt M, Nishioka C, Turner N, Richardson RT, Ericksen T (2014) Monitoring tropical alpine lake levels in a culturally sensitive environment utilizing 3D technological approaches. Arct Antarct Alp Res 46:709–718

Depczynski M, Bellwood DR (2004) Microhabitat utilisation patterns in cryptobenthic coral reef fish communities. Mar Biol 145:

Dewi C, Chen R-C Random forest and support vector machine on features selection for regression analysis. 11

Dinsdale EA, Harriott VJ (2004) Assessing Anchor Damage on Coral Reefs: A Case Study in Selection of Environmental Indicators. Environ Manage 33:126–139

Done T (1992) Done (1992) Phase shifts in coral reef communities and their ecological significance.pdf.

Doney SC, Fabry VJ, Feely RA, Kleypas JA (2009) Ocean Acidification: The Other CO 2 Problem . Annu Rev Mar Sci 1:169–192

Dorenbosch M, Grol M, Christianen M, Nagelkerken I, van der Velde G (2005) Indo-Pacific seagrass beds and mangroves contribute to fish density and diversity on adjacent coral reefs. Mar Ecol Prog Ser 302:63–76

Dubinsky Z, Stambler N (1996) Marine pollution and coral reefs. Glob Change Biol 2:511–526

Dustan P, Doherty O, Pardede S (2013) Digital Reef Rugosity Estimates Coral Reef Habitat Complexity. PLoS ONE 8:e57386

Eakin CM, Liu G, Gomez AM, Geiger EF, Tirak KV, Strong AE (2016) Global Coral Bleaching 2014-2017. 31:6

Echeverry-Galvis MA, Peterson JK, Sulo-Caceres R (2014) The Social Nestwork: Tree Structure Determines Nest Placement in Kenyan Weaverbird Colonies. PLoS ONE 9:e88761

Edinger EN, Risk MJ (2000) Reef classification by coral morphology predicts coral reef conservation value. Biol Conserv 13

Ellison AM (2019) Foundation Species, Non-trophic Interactions, and the Value of Being Common. iScience 13:254–268

English D, Wilkinson CR (1994) Monitoring coral reefs for global change.

Fabricius KE, De'ath G, Noonan S, Uthicke S (2014) Ecological effects of ocean acidification and habitat complexity on reef-associated macroinvertebrate communities. Proc R Soc B Biol Sci 281:20132479

Ferrari R, Bryson M, Bridge T, Hustache J, Williams SB, Byrne M, Figueira W (2016) Quantifying the response of structural complexity and community composition to environmental change in marine communities. Glob Change Biol 22:1965–1975

Ferrari R, Figueira WF, Pratchett MS, Boube T, Adam A, Kobelkowsky-Vidrio T, Doo SS, Atwood TB, Byrne M (2017) 3D photogrammetry quantifies growth and external erosion of individual coral colonies and skeletons. Sci Rep 7:16737

Figueira W, Ferrari R, Weatherby E, Porter A, Hawes S, Byrne M (2015) Accuracy and Precision of Habitat Structural Complexity Metrics Derived from Underwater Photogrammetry. Remote Sens 7:16883–16900

Filbee-Dexter K, Wernberg T (2018) Rise of Turfs: A New Battlefront for Globally Declining Kelp Forests. BioScience 68:64–76

Finstad AG, Einum S, Forseth T, Ugedal O (2007) Shelter availability affects behaviour, size-dependent and mean growth of juvenile Atlantic salmon. Freshw Biol 52:1710–1718

Fontoura L, Zawada KJA, D'agata S, Álvarez-Noriega M, Baird AH, Boutros N, Dornelas M, Luiz OJ, Madin JS, Maina JM, Pizarro O, Torres-Pulliza D, Woods RM, Madin EMP

(2020) Climate-driven shift in coral morphological structure predicts decline of juvenile reef fishes. Glob Change Biol 26:557–567

Fox EW, Hill RA, Leibowitz SG, Olsen AR, Thornbrugh DJ, Weber MH (2017) Assessing the accuracy and stability of variable selection methods for random forest modeling in ecology. Environ Monit Assess 189:316

Fox HE, Pet JS, Dahuri R, Caldwell RL (2003) Recovery in rubble fields: long-term impacts of blast fishing. Mar Pollut Bull 46:1024–1031

Friedlander AM, Parrish JD (1998) Habitat characteristics affecting fish assemblages on a Hawaiian coral reef. J Exp Mar Biol Ecol 224:1–30

Friedman A, Pizarro O, Williams SB, Johnson-Roberson M (2012) Multi-Scale Measures of Rugosity, Slope and Aspect from Benthic Stereo Image Reconstructions. PLoS ONE 7:e50440

Frölicher TL, Laufkötter C (2018) Emerging risks from marine heat waves. Nat Commun 9:650

Fukunaga A, Burns J, Craig B, Kosaki R (2019a) Integrating Three-Dimensional Benthic Habitat Characterization Techniques into Ecological Monitoring of Coral Reefs. J Mar Sci Eng 7:27

Fukunaga A, Burns J, Craig B, Kosaki R (2019b) Integrating Three-Dimensional Benthic Habitat Characterization Techniques into Ecological Monitoring of Coral Reefs. J Mar Sci Eng 7:27

Fukunaga A, Burns JHR (2020) Metrics of Coral Reef Structural Complexity Extracted from 3D Mesh Models and Digital Elevation Models. Remote Sens 12:2676

Fukunaga A, Burns JHR, Pascoe KH, Kosaki RK (2020a) Associations between Benthic Cover and Habitat Complexity Metrics Obtained from 3D Reconstruction of Coral Reefs at Different Resolutions. Remote Sens 12:1011

Fukunaga A, Kosaki RK, Pascoe KH, Burns JHR (2020b) Fish Assemblage Structure in the Northwestern Hawaiian Islands Is Associated with the Architectural Complexity of Coral-Reef Habitats. Diversity 12:430

Gates RD, Ainsworth TD (2011) The nature and taxonomic composition of coral symbiomes as drivers of performance limits in scleractinian corals. J Exp Mar Biol Ecol 408:94–101

Ghadiri Khanaposhtani M, Kaboli M, Karami M, Etemad V (2012) Effect of habitat complexity on richness, abundance and distributional pattern of forest birds. Environ Manage 50:296–303

Glynn PW (1983) Extensive ‘Bleaching’ and Death of Reef Corals on the Pacific Coast of Panamá. Environ Conserv 10:149–154

Glynn PW (1997) Bioerosion and Coral-Reef Growth: A Dynamic Balance. Life and Death of Coral Reefs. Springer US, Boston, MA, pp 68–95

González-Rivero M, Harborne AR, Herrera-Reveles A, Bozec Y-M, Rogers A, Friedman A, Ganase A, Hoegh-Guldberg O (2017) Linking fishes to multiple metrics of coral reef structural complexity using three-dimensional technology. Sci Rep 7:13965

Graham NAJ, Nash KL (2013) The importance of structural complexity in coral reef ecosystems. Coral Reefs 32:315–326

Graham NAJ, Wilson SK, Jennings S, Polunin NVC, Bijoux JP, Robinson J (2006) Dynamic fragility of oceanic coral reef ecosystems. Proc Natl Acad Sci 103:8425–8429

Graham NAJ, Wilson SK, Pratchett MS, Polunin NVC, Spalding MD (2009) Coral mortality versus structural collapse as drivers of corallivorous butterflyfish decline. Biodivers Conserv 18:3325–3336

Gratwicke B, Speight MR (2005a) The relationship between fish species richness, abundance and habitat complexity in a range of shallow tropical marine habitats. J Fish Biol 66:650–667

Gratwicke B, Speight MR (2005b) Effects of habitat complexity on Caribbean marine fish assemblages. Mar Ecol Prog Ser 292:301–310

Guinan J, Brown C, Dolan MFJ, Grehan AJ (2009) Ecological niche modelling of the distribution of cold-water coral habitat using underwater remote sensing data. Ecol Inform 4:83–92

Haisfield KM, Fox HE, Yen S, Mangubhai S, Mous PJ (2010) An ounce of prevention: cost-effectiveness of coral reef rehabilitation relative to enforcement: Coral reef rehabilitation relative to enforcement. Conserv Lett 3:243–250

Harborne AR, Mumby PJ, Ferrari R (2012) The effectiveness of different meso-scale rugosity metrics for predicting intra-habitat variation in coral-reef fish assemblages. Environ Biol Fishes 94:431–442

Harmelin-Vivien ML, Bouchon-Navaro Y (1983) Feeding diets and significance of coral feeding among Chaetodontid fishes in Moorea (French Polynesia). Coral Reefs 2:119–127

Harriott VJ, Dinsdale EA (2004) Assessing Anchor Damage on Coral Reefs: A Case Study in Selection of Environmental Indicators. Environ Manage 33:126–139

Henderson CJ, Gilby BL, Lee SY, Stevens T (2017) Contrasting effects of habitat complexity and connectivity on biodiversity in seagrass meadows. Mar Biol 164:117

Hennige SJ, Burdett HL, Perna G, Tudhope AW, Kamenos NA (2017) The potential for coral reef establishment through free-living stabilization. Sci Rep 7:13322

Heron SF, Maynard JA, van Hooidonk R, Eakin CM (2016) Warming Trends and Bleaching Stress of the World's Coral Reefs 1985–2012. Sci Rep 6:38402

Hill J, Wilkinson C (2004) Methods for Ecological Monitoring of Coral Reefs: Version 1. Australian Institute of Marine Science, Townsville

Hixon MA, Beets JP (1993) Predation, Prey Refuges, and the Structure of Coral-Reef Fish Assemblages. Ecol Monogr 63:77–101

Hoegh-Guldberg O (1999) Climate change, coral bleaching and the future of the world's coral reefs. Mar Freshw Res

Hoegh-Guldberg O (2011) Coral reef ecosystems and anthropogenic climate change. Reg Environ Change 11:215–227

Hoegh-Guldberg O, Mumby PJ, Hooten AJ, Steneck RS, Greenfield P, Gomez E, Harvell CD, Sale PF, Edwards AJ, Caldeira K, Knowlton N, Eakin CM, Iglesias-Prieto R, Muthiga N, Bradbury RH, Dubi A, Hatziolos ME (2007) Coral Reefs Under Rapid Climate Change and Ocean Acidification. Science 318:1737–1742

Hoegh-Guldberg O, Pendleton L, Kaup A (2019) People and the changing nature of coral reefs. Reg Stud Mar Sci 30:

Hoegh-Guldberg O, Salvat B (1995) Periodic mass-bleaching and elevated sea temperatures:bleaching of outer reef slope communities in Moorea, French Polynesia. Mar Ecol Prog Ser 121:181–190

Hohnen R, Tuft K, McGregor HW, Legge S, Radford IJ, Johnson CN (2016) Occupancy of the Invasive Feral Cat Varies with Habitat Complexity. PLOS ONE 11:e0152520

Hughes TP, Anderson KD, Connolly SR, Heron SF, Kerry JT, Lough JM, Baird AH, Baum JK, Berumen ML, Bridge TC, Claar DC, Eakin CM, Gilmour JP, Graham NAJ, Harrison H, Hobbs J-PA, Hoey AS, Hoogenboom M, Lowe RJ, McCulloch MT, Pandolfi JM, Pratchett M, Schoepf V, Torda G, Wilson SK (2018a) Spatial and temporal patterns of mass bleaching of corals in the Anthropocene. Science 359:80–83

Hughes TP, Baird AH, Bellwood DR, Card M, Connolly SR, Folke C, Grosberg R, Hoegh-Guldberg O, Jackson JBC, Kleypas J, Lough JM, Marshall P, Nyström M, Palumbi SR, Pandolfi JM, Rosen B, Roughgarden J (2003) Climate change, human impacts, and the resilience of coral reefs. Science 301:929–933

Hughes TP, Kerry JT, Álvarez-Noriega M, Álvarez-Romero JG, Anderson KD, Baird AH, Babcock RC, Beger M, Bellwood DR, Berkelmans R, Bridge TC, Butler IR, Byrne M, Cantin NE, Comeau S, Connolly SR, Cumming GS, Dalton SJ, Diaz-Pulido G, Eakin CM, Figueira WF, Gilmour JP, Harrison HB, Heron SF, Hoey AS, Hobbs J-PA, Hoogenboom MO, Kennedy EV, Kuo C, Lough JM, Lowe RJ, Liu G, McCulloch MT, Malcolm HA, McWilliam MJ, Pandolfi JM, Pears RJ, Pratchett MS, Schoepf V, Simpson

T, Skirving WJ, Sommer B, Torda G, Wachenfeld DR, Willis BL, Wilson SK (2017) Global warming and recurrent mass bleaching of corals. Nature 543:373–377

Hughes TP, Kerry JT, Baird AH, Connolly SR, Dietzel A, Eakin CM, Heron SF, Hoey AS, Hoogenboom MO, Liu G, McWilliam MJ, Pears RJ, Pratchett MS, Skirving WJ, Stella JS, Torda G (2018b) Global warming transforms coral reef assemblages. Nature 556:492–496

Hunt CL, Kelly GR, Windmill H, Curtis-Quick J, Conlon H, Bodmer MDV, Rogers AD, Exton DA (2019) Aggregating behaviour in invasive Caribbean lionfish is driven by habitat complexity. Sci Rep 9:783

Hutchings PA (1986) Biological destruction of coral reefs - A review. Coral Reefs 4:239–252

IPCC (2019) IPCC Special Report on the Ocean and Cryosphere in a Changing Climate.

Javernick L, Brasington J, Caruso B (2014) Modeling the topography of shallow braided rivers using Structure-from-Motion photogrammetry. Geomorphology 213:166–182

Johnson MP, Frost NJ, Mosley MWJ, Roberts MF, Hawkins SJ (2003) The area-independent effects of habitat complexity on biodiversity vary between regions. Ecol Lett 6:126–132

Jones CG, Lawton JH, Shachak M (1994) Organisms as Ecosystem Engineers. Oikos 69:373

Jones GP, McCormick MI, Srinivasan M, Eagle JV (2004) Coral decline threatens fish biodiversity in marine reserves. Proc Natl Acad Sci 101:8251–8253

Kayanne H (2017) Validation of degree heating weeks as a coral bleaching index in the northwestern Pacific. Coral Reefs 36:63–70

Knudby A, LeDrew E (2007) Measuring Structural Complexity on Coral Reefs. 8

Kostylev VE, Erlandsson J, Ming MY, Williams GA (2005) The relative importance of habitat complexity and surface area in assessing biodiversity: Fractal application on rocky shores. Ecol Complex 2:272–286

Kovalenko KE, Thomaz SM, Warfe DM (2012) Habitat complexity: Approaches and future directions. Hydrobiologia 685:1–17

Kramer M, Bellwood D, Bellwood O (2014) Benthic Crustacea on coral reefs: a quantitative survey. Mar Ecol Prog Ser 511:105–116

Lamb JB, True JD, Piromvaragorn S, Willis BL (2014) Scuba diving damage and intensity of tourist activities increases coral disease prevalence. Biol Conserv 178:88–96

Lassau SA, Hochuli DF, Cassis G, Reid CAM (2005) Lassau et al, 2005. Divers Distrib 11:73–82

Lavy A, Eyal G, Neal B, Keren R, Loya Y, Ilan M (2015) A quick, easy and non-intrusive method for underwater volume and surface area evaluation of benthic organisms by 3D computer modelling. Methods Ecol Evol 6:521–531

Lee J-H, Sull S (2019) Regression Tree CNN for Estimation of Ground Sampling Distance Based on Floating-Point Representation. 17

Leggat WP, Camp EF, Suggett DJ, Heron SF, Fordyce AJ, Gardner S, Deakin L, Turner M, Beeching LJ, Kuzhiumparambil U, Eakin CM, Ainsworth TD (2019) Rapid Coral Decay Is Associated with Marine Heatwave Mortality Events on Reefs. Curr Biol 29:2723-2730.e4

Lenth R (2017) emmeans: Estimated Marginal Means, aka Least-Squares Means. The American Statistician

Leon JX, Roelfsema CM, Saunders MI, Phinn SR (2015) Measuring coral reef terrain roughness using ‘Structure-from-Motion’ close-range photogrammetry. Geomorphology 242:21–28

Liaw A, Wiener M (2002) Classification and Regression by randomForest. 2:6

Liu G, Heron S, Eakin C, Muller-Karger F, Vega-Rodriguez M, Guild L, De La Cour J, Geiger E, Skirving W, Burgess T, Strong A, Harris A, Maturi E, Ignatov A, Sapper J, Li J, Lynds S (2014) Reef-Scale Thermal Stress Monitoring of Coral Ecosystems: New 5-km Global Products from NOAA Coral Reef Watch. Remote Sens 6:11579–11606

Loya Y, Sakai K, Yamazato K, Nakano Y, Sambali H, Woesik R van (2001) Coral bleaching: the winners and the losers. Ecol Lett 4:122–131

Luckhurst BE, Luckhurst K (1978) Analysis of the influence of substrate variables on coral reef fish communities. Mar Biol 49:317–323

MacArthur RH, MacArthur JW (1961) On Bird Species Diversity. Ecology 42:594–598

Magel JMT, Burns JHR, Gates RD, Baum JK (2019) Effects of bleaching-associated mass coral mortality on reef structural complexity across a gradient of local disturbance. Sci Rep 9:2512

Magel JMT, Dimoff SA, Baum JK (2020) Direct and indirect effects of climate change-amplified pulse heat stress events on coral reef fish communities. Ecol Appl 30:

Mandelbrot BB (1982) Mandelbrot (1982) The Fractal Geometry of Nature.pdf.

Mann KH (1973) Mann (1973) Seaweeds_ Their Productivity and Strategy for Growth.pdf. Science 182:975–981

McCormick M (1994) Comparison of field methods for measuring surface topography and their associations with a tropical reef fish assemblage. Mar Ecol Prog Ser 112:87–96

McDevitt-Irwin JM, Garren M, McMinds R, Vega Thurber R, Baum JK (2019) Variable interaction outcomes of local disturbance and El Niño-induced heat stress on coral microbiome alpha and beta diversity. Coral Reefs 38:331–345

McGregor H, Legge S, Jones ME, Johnson CN (2015) Feral cats are better killers in open habitats, revealed by animal-borne video. PLoS ONE 10:1–12

McManus JW, Polsenberg JF (2004) Coral–algal phase shifts on coral reefs: Ecological and environmental aspects. Prog Oceanogr 60:263–279

Moberg F, Folke C (1999) Ecological goods and services of coral reef ecosystems. Ecol Econ 29:215–233

Mumby PJ, Harborne AR, Williams J, Kappel C V., Brumbaugh DR, Micheli F, Holmes KE, Dahlgren CP, Paris CB, Blackwell PG (2007) Trophic cascade facilitates coral recruitment in a marine reserve. Proc Natl Acad Sci U S A 104:8362–8367

Oakley-Cogan A, Tebbett SB, Bellwood DR (2020) Habitat zonation on coral reefs: Structural complexity, nutritional resources and herbivorous fish distributions. PLOS ONE 15:e0233498

Oliver ECJ, Benthuysen JA, Darmaraki S, Donat MG, Hobday AJ, Holbrook NJ, Schlegel RW, Sen Gupta A (2021) Marine Heatwaves. Annu Rev Mar Sci 13:313–342

Oliver ECJ, Donat MG, Burrows MT, Moore PJ, Smale DA, Alexander LV, Benthuysen JA, Feng M, Sen Gupta A, Hobday AJ, Holbrook NJ, Perkins-Kirkpatrick SE, Scannell HA, Straub SC, Wernberg T (2018) Longer and more frequent marine heatwaves over the past century. Nat Commun 9:1324

Perry CT, Alvarez-Filip L (2018) Changing geo-ecological functions of coral reefs in the Anthropocene. Funct Ecol 1365-2435.13247

Pittman SJ, Costa BM, Battista TA (2009) Using Lidar Bathymetry and Boosted Regression Trees to Predict the Diversity and Abundance of Fish and Corals. J Coast Res 10053:27–38

Polunin N, Roberts C (1993) Greater biomass and value of target coral-reef fishes in two small Caribbean marine reserves. Mar Ecol Prog Ser 100:167–176

Prasad AM, Iverson LR, Liaw A (2006) Newer Classification and Regression Tree Techniques: Bagging and Random Forests for Ecological Prediction. Ecosystems 9:181–199

Pratchett M, Anderson K, Hoogenboom M, Widman E, Baird A, Pandolfi J, Edmunds P, Lough J (2015) Spatial, Temporal and Taxonomic Variation in Coral Growth—Implications for the Structure and Function of Coral Reef Ecosystems. Oceanogr Mar Biol 215–296

Pratchett MS (2005) Dietary overlap among coral-feeding butterflyfishes (Chaetodontidae) at Lizard Island, northern Great Barrier Reef. Mar Biol 148:373–382

Pratchett MS, Hoey AS, Wilson SK, Messmer V, Graham NAJ (2011) Changes in biodiversity and functioning of reef fish assemblages following coral bleaching and coral loss. Diversity 3:424–452

R Core Team (2019) R: A language and environment for statistical computing. R Found Stat Comput Vienna Austria 16

Raymundo LJ, Maypa AP, Gomez ED, Cadiz P (2007) Can dynamite-blasted reefs recover? A novel, low-tech approach to stimulating natural recovery in fish and coral populations. Mar Pollut Bull 54:1009–1019

Reaka-Kudla ML (1997) The Global Biodiversity of Coral Reefs: A Comparison with Rain Forests. 26

Reed JK, Koenig CC, Shepard AN (2007) Impacts of bottom trawling on a deep-water Oculina coral ecosystem off Florida. Bull Mar Sci 81:481–496

Reichert J, Backes AR, Schubert P, Wilke T (2017) The power of 3D fractal dimensions for comparative shape and structural complexity analyses of irregularly shaped organisms. Methods Ecol Evol 8:1650–1658

Risk MJ (1972) Fish diversity on a coral reef in the Virgin Islands. Atoll Res Bull 1–6

Roberts CM (1995) Effects of Fishing on the Ecosystem Structure of Coral Reefs Published by : Wiley for Society for Conservation Biology. Soc Conserv Biol 9:988–995

Rogers C (1990) Responses of coral reefs and reef organisms to sedimentation. Mar Ecol Prog Ser 62:185–202

Sappington JM, Longshore KM, Thompson DB (2007) Quantifying Landscape Ruggedness for Animal Habitat Analysis: A Case Study Using Bighorn Sheep in the Mojave Desert. J Wildl Manag 71:1419–1426

Sebens KP (1994) Biodiversity of Coral Reefs: What are We Losing and Why? Am Zool 34:115–133

Sheppard CRC, Spalding M, Bradshaw C, Wilson S (2002) Erosion vs. Recovery of Coral Reefs after 1998 El Niño: Chagos Reefs, Indian Ocean. AMBIO J Hum Environ 31:40–48

Simon T, Joyeux JC, Pinheiro HT (2013) Fish assemblages on shipwrecks and natural rocky reefs strongly differ in trophic structure. Mar Environ Res 90:55–65

Spalding M, Burke L, Wood SA, Ashpole J, Hutchison J, zu Ermgassen P (2017) Mapping the global value and distribution of coral reef tourism. Mar Policy 82:104–113

Steneck RS, Graham MH, Bourque BJ, Corbett D, Erlandson JM, Estes JA, Tegner MJ (2002) Kelp forest ecosystems: Biodiversity, stability, resilience and future. Environ Conserv 29:436–459

Steneck RS, Johnson CR (2013) Dynamic Patterns, Processes, and Feedbacks. 23

Stoddart DR (1969) Ecology and morphology of recent coral reefs. Biol Rev 44:433–498

Storlazzi CD, Dartnell P, Hatcher GA, Gibbs AE (2016) End of the chain? Rugosity and fine-scale bathymetry from existing underwater digital imagery using structure-from-motion (SfM) technology. Coral Reefs 35:889–894

Strobl C, Boulesteix A-L, Kneib T, Augustin T, Zeileis A (2008) Conditional variable importance for random forests. BMC Bioinformatics 9:307

Swirad ZM, Rosser NJ, Brain MJ (2019) Identifying mechanisms of shore platform erosion using Structure-from-Motion (SfM) photogrammetry. Earth Surf Process Landf 44:1542–1558

Talmage SC, Gobler CJ (2010) Effects of past, present, and future ocean carbon dioxide concentrations on the growth and survival of larval shellfish. Proc Natl Acad Sci U S A 107:17246–17251

Teagle H, Hawkins SJ, Moore PJ, Smale DA (2017) The role of kelp species as biogenic habitat formers in coastal marine ecosystems. J Exp Mar Biol Ecol 492:81–98

Todd PA (2008) Morphological plasticity in scleractinian corals. Biol Rev 83:315–337

Torda G, Sambrook K, Cross P, Sato Y, Bourne DG, Lukoschek V, Hill T, Torras Jorda G, Moya A, Willis BL (2018) Decadal erosion of coral assemblages by multiple disturbances in the Palm Islands, central Great Barrier Reef. Sci Rep 8:11885

Torres-Pulliza D, Dornelas MA, Pizarro O, Bewley M, Blowes SA, Boutros N, Brambilla V, Chase TJ, Frank G, Friedman A, Hoogenboom MO, Williams S, Zawada KJA, Madin JS (2020) A geometric basis for surface habitat complexity and biodiversity. Nat Ecol Evol 4:1495–1501

Vargas-Ángel B, Huntington B, Brainard RE, Venegas R, Oliver T, Barkley H, Cohen A (2019) El Niño-associated catastrophic coral mortality at Jarvis Island, central Equatorial Pacific. Coral Reefs 38:731–741

Vaughan T, Wells J (1943) Revision of the Suborders Families, and Genera of the Scleractinia. Geological Society of America,

Vermeij MJA (2006) Early life-history dynamics of Caribbean coral species on artificial substratum: The importance of competition, growth and variation in life-history strategy. Coral Reefs 25:59–71

Veron J (2000) Corals of the world (Veron, 2000).pdf. Townsville, Darwin, Perth: Australian Institute of Marine Sceince

Veron J (2013) Overview of the taxonomy of zooxanthellate Scleractinia: Overview of Coral Taxonomy. Zool J Linn Soc 169:485–508

Walbridge S, Slocum N, Pobuda M, Wright D (2018) Unified Geomorphological Analysis Workflows with Benthic Terrain Modeler. Geosciences 8:94

Warfe DM, Barmuta LA (2004) Habitat structural complexity mediates the foraging success of multiple predator species. Oecologia 141:171–178

Watson MS, Claar DC, Baum JK (2016) Subsistence in isolation: Fishing dependence and perceptions of change on Kiritimati, the world's largest atoll. Ocean Coast Manag 123:1–8

Westoby MJ, Brasington J, Glasser NF, Hambrey MJ, Reynolds JM (2012) "Structure-from-Motion" photogrammetry: A low-cost, effective tool for geoscience applications. Geomorphology 179:300–314

Wickham H (2016) ggplot2: Elegant Graphics for Data Analysis.

Wilson SK, Fisher R, Pratchett MS, Graham NAJ, Dulvy NK, Turner RA, Cakacaka A, Polunin NVC (2010) Habitat degradation and fishing effects on the size structure of coral reef fish communities. Ecol Appl 20:442–451

Wilson SK, Graham NAJ, Polunin NVC (2007) Appraisal of visual assessments of habitat complexity and benthic composition on coral reefs. Mar Biol 151:1069–1076

Wilson SK, Graham NAJ, Pratchett MS, Jones GP, Polunin NVC (2006) Multiple disturbances and the global degradation of coral reefs: Are reef fishes at risk or resilient? Glob Change Biol 12:2220–2234

Young GC, Dey S, Rogers AD, Exton D (2017) Cost and time-effective method for multi-scale measures of rugosity, fractal dimension, and vector dispersion from coral reef 3D models. PLOS ONE 12:e0175341

Zawada KJA, Dornelas M, Madin JS (2019) Quantifying coral morphology. Coral Reefs 38:1281–1292

Tables and Figures

Table 2.1 Top model sets describing each habitat metric at 1.0cm DEM resolution. All models are within Δ4AIC$_c$, with degrees of freedom (df), AIC corrected (), and model weight (*w*) reported. Disturbance = continuous gradient of local anthropogenic disturbance, Year*Disturbance = presence of an interaction term between year and disturbance level; Site Exposure = exposure of site to different hypothesized wave energy levels based on geographic location.

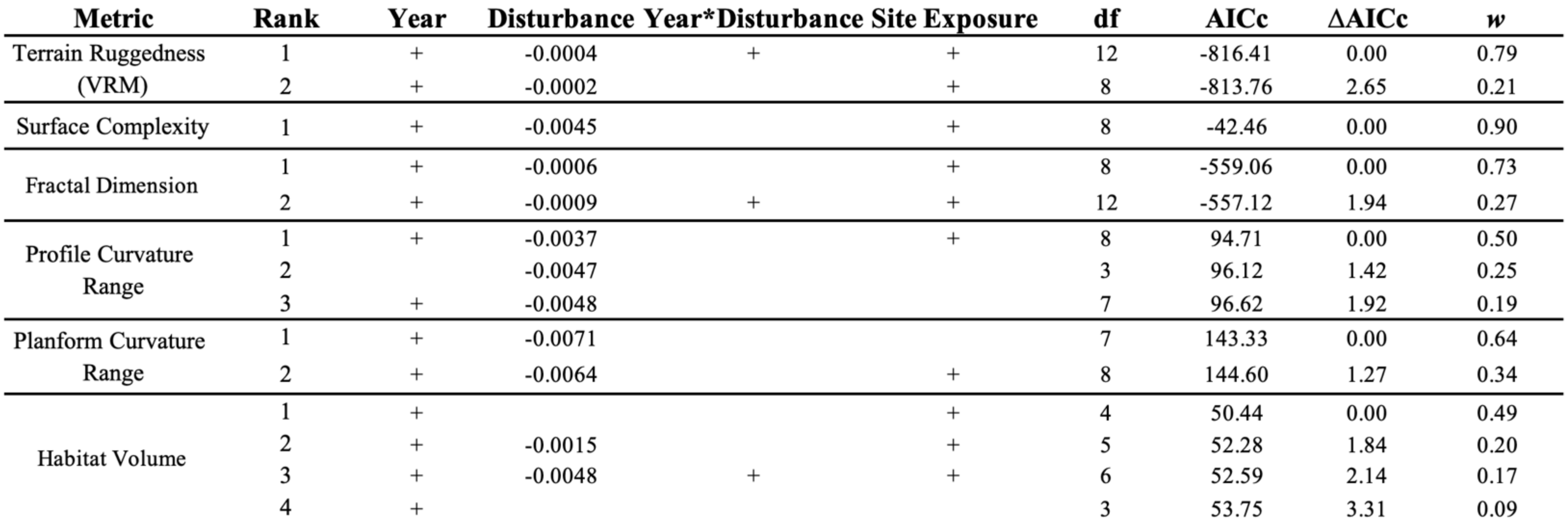

Metric	Rank	Year	Disturbance	Year*Disturbance	Site Exposure	df	AICc	ΔAICc	*w*
Terrain Ruggedness (VRM)	1	+	-0.0004	+	+	12	-816.41	0.00	0.79
	2	+	-0.0002		+	8	-813.76	2.65	0.21
Surface Complexity	1	+	-0.0045		+	8	-42.46	0.00	0.90
Fractal Dimension	1	+	-0.0006		+	8	-559.06	0.00	0.73
	2	+	-0.0009	+	+	12	-557.12	1.94	0.27
Profile Curvature Range	1	+	-0.0037		+	8	94.71	0.00	0.50
	2		-0.0047			3	96.12	1.42	0.25
	3	+	-0.0048			7	96.62	1.92	0.19
Planform Curvature Range	1	+	-0.0071			7	143.33	0.00	0.64
	2	+	-0.0064		+	8	144.60	1.27	0.34
Habitat Volume	1	+			+	4	50.44	0.00	0.49
	2	+	-0.0015		+	5	52.28	1.84	0.20
	3	+	-0.0048	+	+	6	52.59	2.14	0.17
	4	+				3	53.75	3.31	0.09

Table 2.2 Top morphological predictors of each habitat structure metric at 1cm resolution using the full, complex classification with the default random forest *mtry* settings.

Habitat Metric	**Mean of square residuals**	**Variance Explained (%)**	**Top 5 predictor variables**	
			%IncMSE	**IncNodePurity**
VRM	0.000119	57.18	1. Live Submassive	1. Live Branching
			2. Live Branching	2. Live Submassive
			3. Live Foliose	3. Live Foliose
			4. Live Encrusting	4. Live Tabulate
			5. Live Tabulate	5. Rubble
Surface Complexity	0.04078	49.9	1. Live Submassive	1. Live Submassive
			2. Live Tabulate	2. Live Tabulate
			3. Live Porites	3. Live Branching
			4. Live Branching	4. Live Foliose
			5. Live Foliose	5. Rubble
Fractal Dimension	0.0009511	53.38	1. Live Foliose	1. Live Foliose
			2. Dead Tabulate	2. Live Branching
			3. Dead Branching	3. Live Submassive
			4. Live Branching	4. Dead Branching
			5. Live Submassive	5. Dead Foliose
Profile Curvature Range	0.103	9.83	1. Dead Branching	1. Dead Branching
			2. Live Porites	2. Live Porites
			3. Live Branching	3. Live Branching
			4. Live Encrusting Collumnar	4. Live Encrusting
			5. Live Tabulate	5 Live Submassive
Plandform Curvature Range	0.1444	10.4	1. Live Branching	1. Live Branching
			2. Live Submassive	2. Live Encrusting
			3. Live Tabulate	3. Live Porites
			4. Live Porites	4. Live Submassive
			5. Macroalgae	5. Live Massive

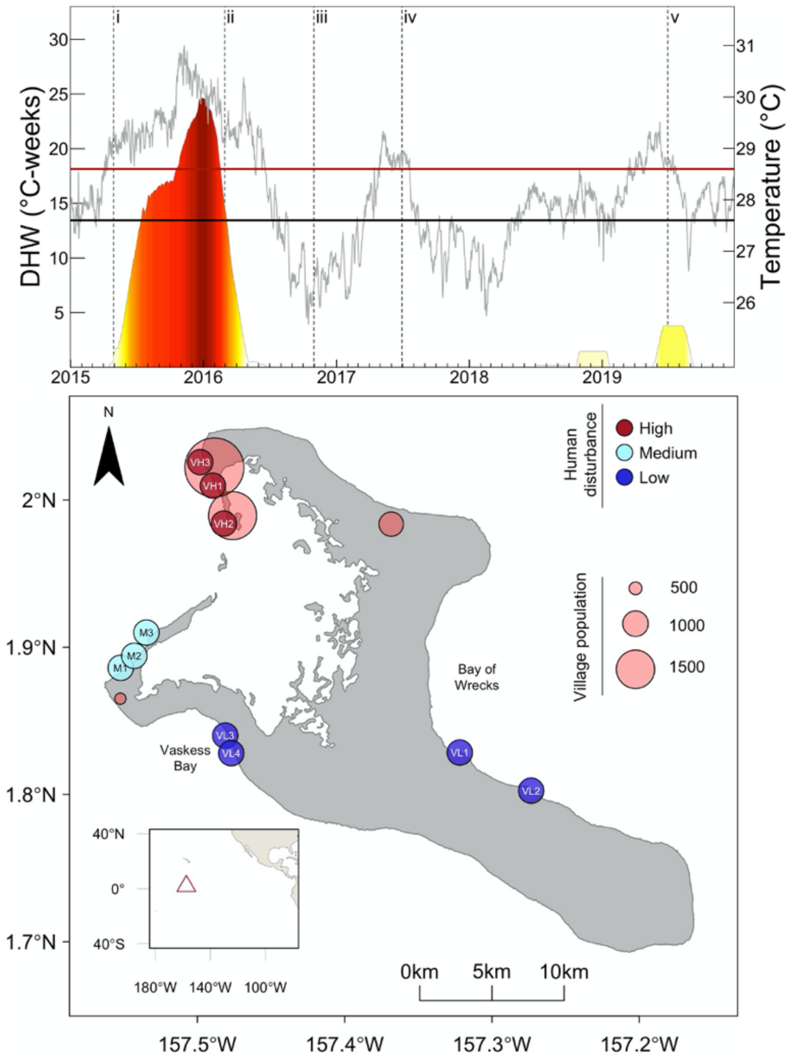

Figure 2.1 Marine heatwave development (top) reprinted with permission from Claar et al. (2020) showing NOAA satellite temperature data from around Kiritimati (gray line), maximum monthly mean (horizontal black line), and bleaching threshold (horizontal red line; right axis). Colored shading indicates cumulative heat stress levels (DHW; left axis) according to coral thermal thresholds: NOAA Coral Reef Watch Bleaching Alert 1 (yellow) and 2 (orange), "mass coral mortality" expected (red) and "not experienced by reefs" (black). Map (bottom) of Kiritimati showing forereef sites sampled categorized by local anthropogenic disturbance. Sites are divided into three levels of local disturbance, with villages (red circles) scaled to the human population size present and the inset shows Kiritimati's location in the equatorial Pacific Ocean**.**

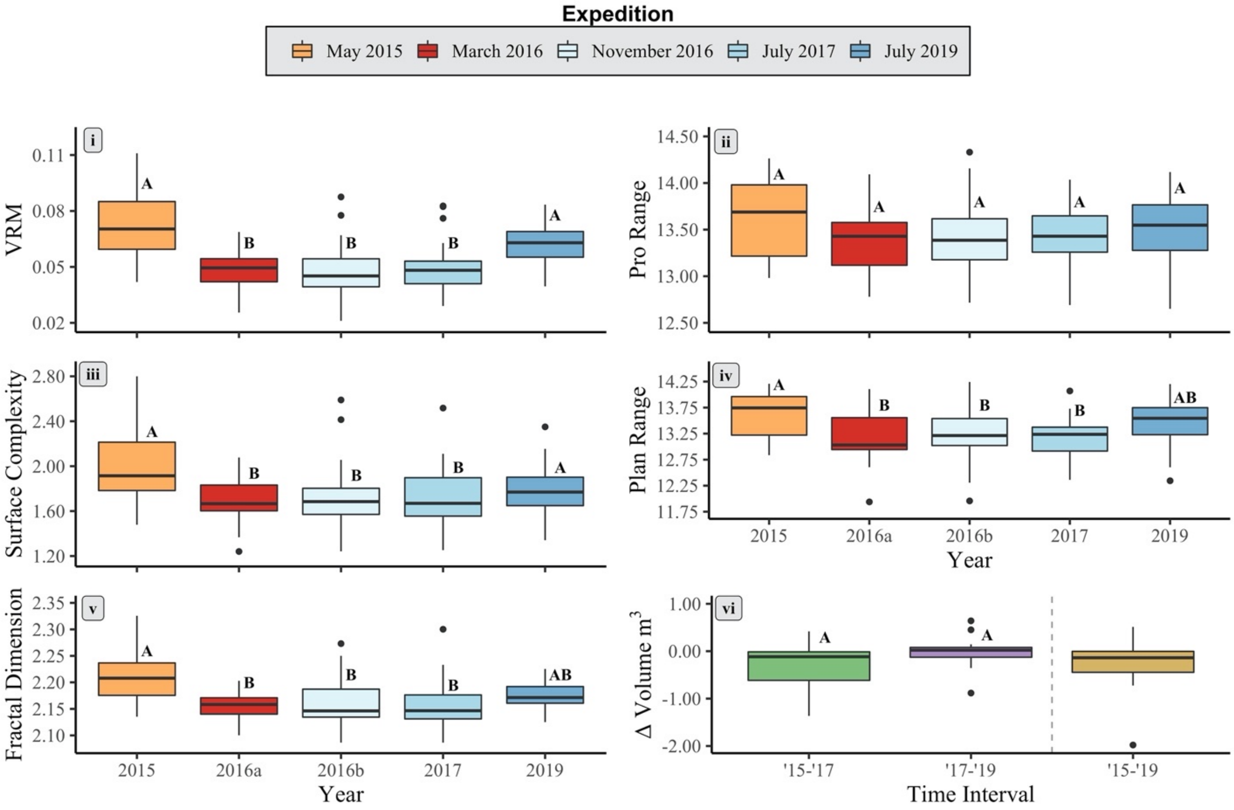

Figure 2.2 Habitat structure metrics captured from before just prior to the heatwave (May 2015), immediately post (March 2016a), 7 months post (November 2016b), 15 months post (July 2017), and nearly 3 years post (July 2019). Structural complexity metrics sampled include metrics of complexity (i. Terrain Ruggedness (VRM), iii. Surface Complexity, v. Fractal Dimension), curvature range (ii. Profile Curvature Range, iv. Planform Curvature Range), and vi. Habitat Volumetric Change. Statistically significant yearly differences computed via Tukey pairwise post-hoc analyses are indicated by the letters A and B above each boxplot.

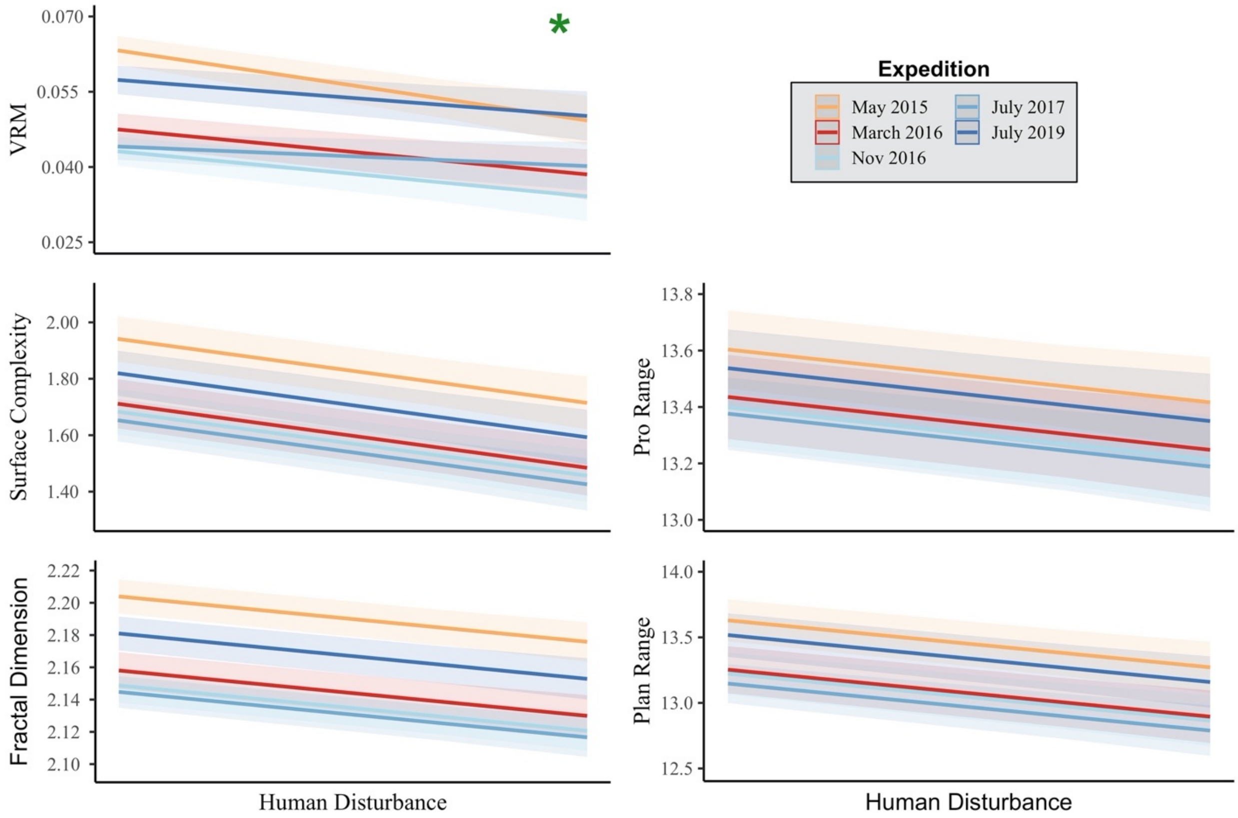

Figure 2.3 Habitat Structure metric's predicted values at 1.0 cm DEM resolution across the gradient of local anthropogenic disturbance from all five expeditions. The green star indicates a significant interaction present between local disturbance and year.

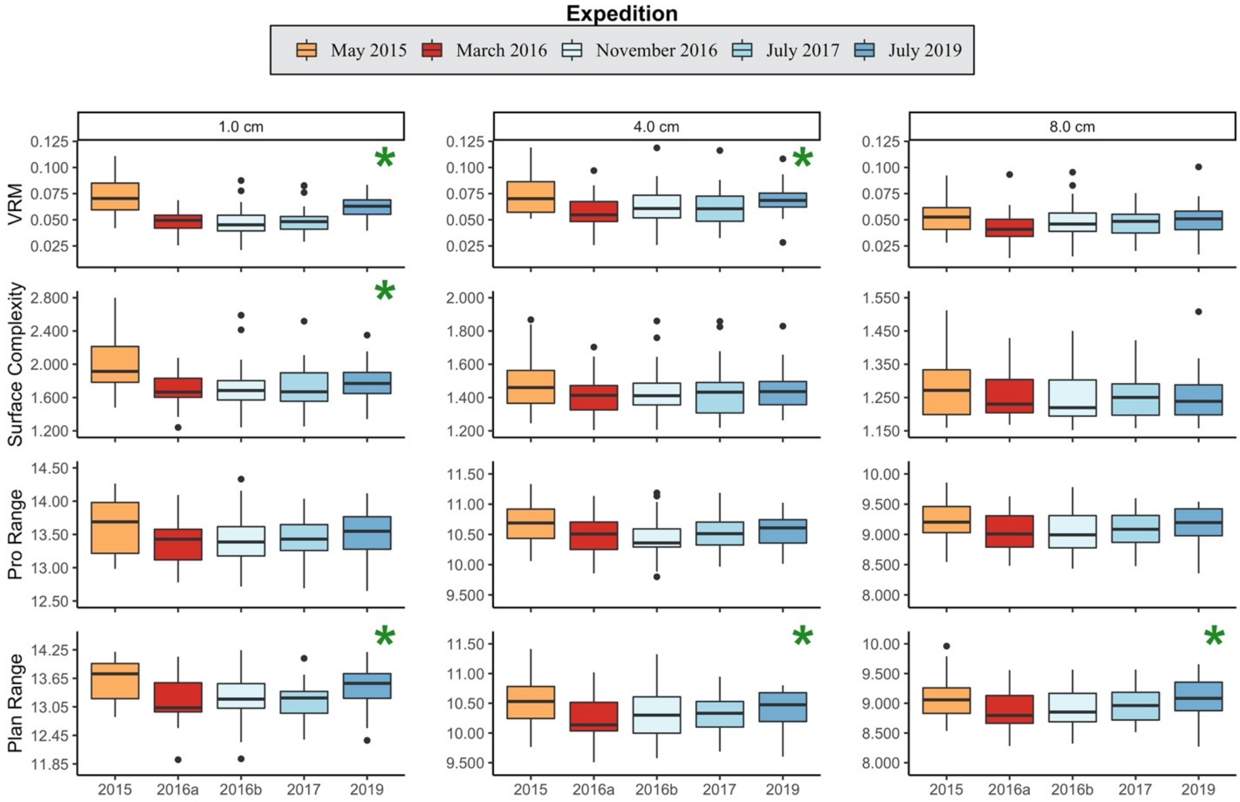

Figure 2.4 Habitat complexity metrics (terrain ruggedness (VRM), surface complexity, log-transformed profile curvature range (Pro Range), and log-transformed planform curvature range (Plan Range)) across the three resolution scales (1.0, 4.0, 8.0 cm) documented in this study. Green stars indicate yearly significance present at that specific resolution scale.

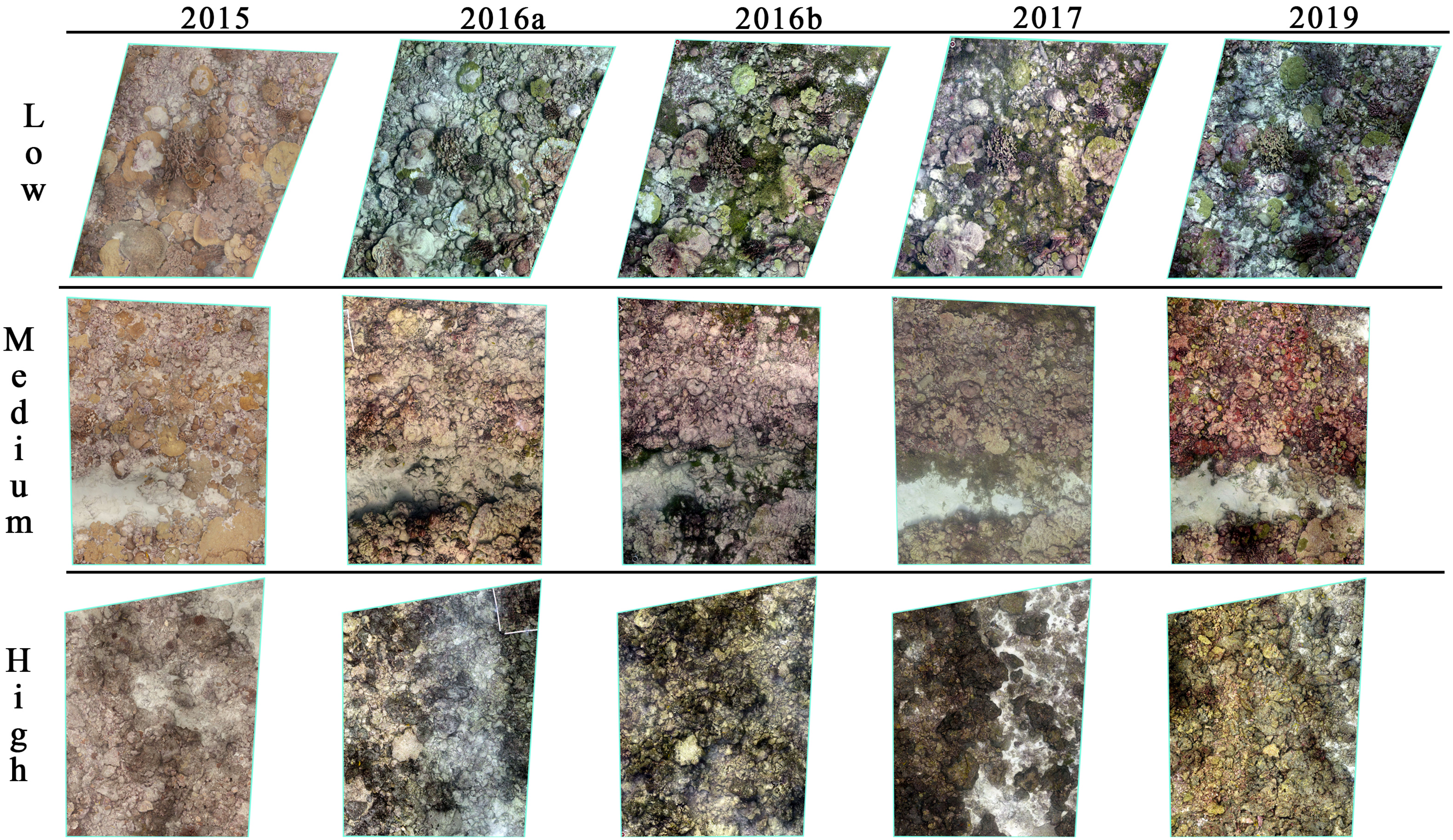

Figure 2.5 PPQ timeseries showing plot changes throughout the study across low, medium, and high levels of local anthropogenic disturbance

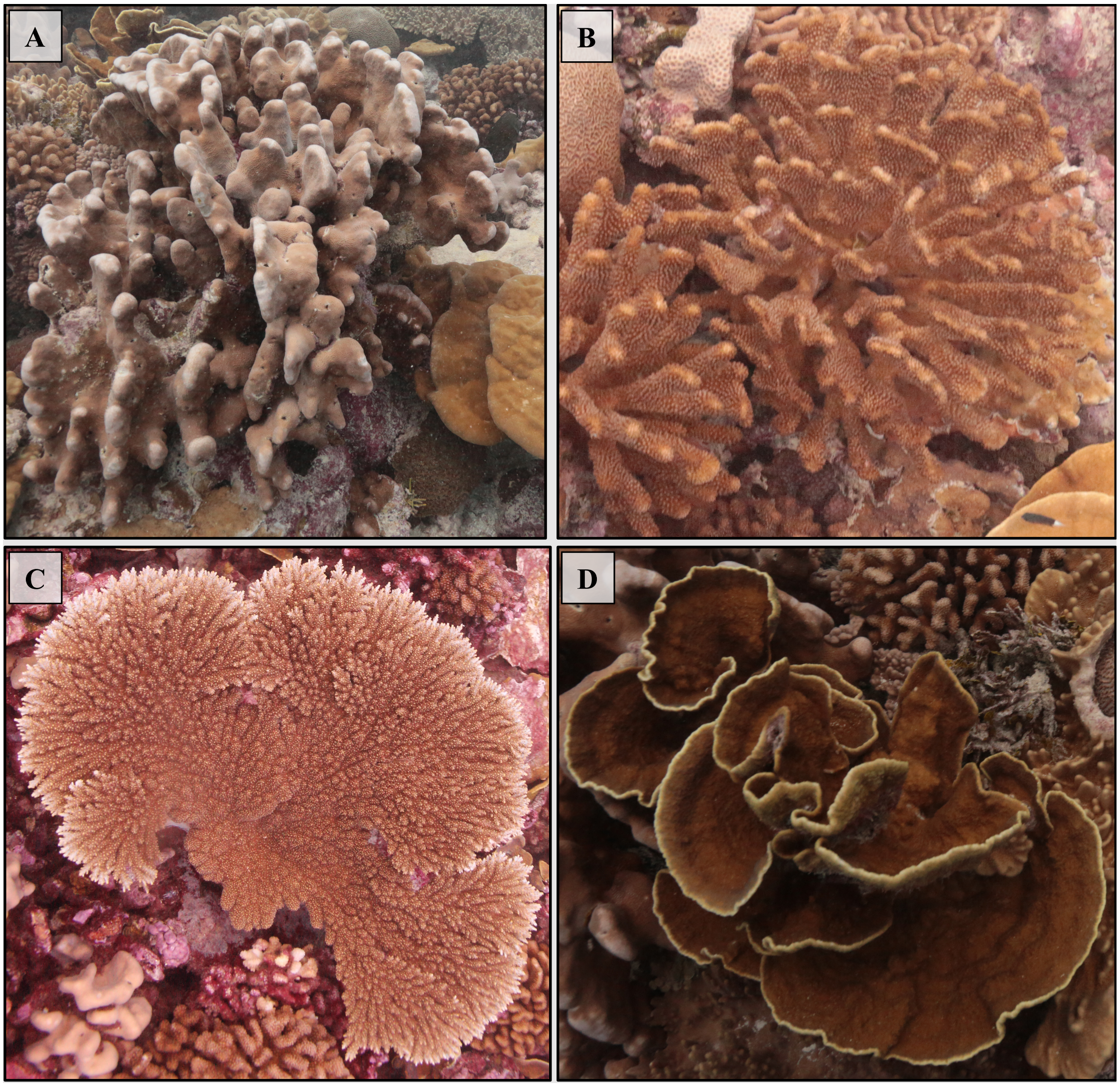

Figure 2.6 Top morphological predictors of habitat complexity: A. Submassive, B. Branching, C. Tabulate, and D. Foliose.

Appendices

Appendix A: Supplemental information for Chapter 2

Table A.2.1 Total amount of PPQ's sampled during each of the five expeditions.

Site	***Disturbance***	Pre-El Niño	End of heatstress	9 months post	1 year post	3 years post	***Total***
		May '15	***March '16***	***Nov '16***	***July '17***	***July '19***	
27	Very High	3	3	3	3	3	15
30		3	3	3	3	3	15
32		3	3	3	3	3	15
8	Medium	3	3	3	3	3	15
34		3	3	3	3	3	15
35		3	2	3	3	3	14
5	Very Low	3	3	3	3	3	15
15		3	1	3	3	0	10
19		2	0	2	3	0	7
37		0	0	0	3	3	6

Table A.2.2 Top model sets describing each habitat structure metric at 4.0 and 8.0cm DEM resolutions. All models are within Δ4AICc, the degrees of freedom (df), AIC corrected (AICc) and model weight (*w*) reported.

Metric	Rank	Resolution	Year	Disturbance	Year*Disturbance	Site Exposure	df	LL	AICc	ΔAICc	*w*
Terrain Ruggedness (VRM)	1	4cm	+	-0.000244815		+	8	367.90	-718.57	0.00	0.95
	1	8cm	+	-0.00030001		+	8	372.81	-728.41	0.00	0.56
	2			-0.000343004			3	366.46	-726.73	1.68	0.24
	3		+	-0.00034515			7	370.53	-726.12	2.29	0.18
Surface Complexity	1	4cm	+	-0.00273115		+	8	82.76	-148.29	0.00	0.41
	2		+				7	81.52	-148.10	0.19	0.38
	3			-0.003237226			3	76.03	-145.86	2.43	0.12
	4		+	-0.003242113			7	79.74	-144.53	3.76	0.06
	1	8cm		-0.00187824			3	133.57	-260.95	0.00	0.81
Profile Curvature Range	1	4cm	+	-0.002575399		+	8	-22.52	62.26	0.00	0.72
	1	8cm	+				7	-22.15	59.24	0.00	0.70
	2			-0.004052705			3	-28.25	62.70	3.45	0.12
	3		+	-0.004088749			7	-23.99	62.93	3.69	0.11
Planform Curvature Range	1	4cm	+	-0.004048347		+	8	-33.97	85.15	0.00	0.63
	2		+	-0.005151366			7	-36.22	87.38	2.22	0.21
	1	8cm	+	-0.004751396			7	-22.03	59.00	0.00	0.56
	2			-0.004717089			3	-27.36	60.92	1.92	0.21
	3		+	-0.004768264		+	8	-22.03	61.28	2.28	0.18

Table A.2.3 Coral morphological classification. Columns indicate simple and complex morphological classifications for all structural components analyzed in this study, with taxonomic group (Order), and possible species list.

Simple Classification	Complex Classification	Taxonomic Group	Possible species include
Branching	Live_Branching	Acroporidae, Pocilloporidae	*Acropora globiceps, Acropora loripes,Acropora gemmifera, Acropora loripes x subulata (hybrid), Acropora subulata, Pocillopora zelli, Pocillopora grandis, Pocillopora meandrina*
	NonCoral_Branching	Stylasteridae	*Stylaster sp*
Massive	Live_Columnar	Merulinidae	*Dipsastraea matthaii*
	Live_Encrusting	Acroporidae, Merulinidae, Agariciidae, Psammocoridae, Dendrophylliidae	*Astrea annuligera, Astrea curta, Astreopora cucullata, Astreopera suggesta, Coscinaraea spp., Favites halicora, Gardineroseris planulata, Leptastrea bewickensis, Leptastrea pruinosa, Leptastrea purpurea, Leptastrea pruinosa, Montipora spp.,Pavona varians, Psammocora profundacella, Turbinaria stellulata, Leptoseris mycetoseroides*
	Live_FreeLiving	Fungiidae	*Cycloseris tenuis, Cycloseris fagilis, Lithophyllon, Danafungia scruposa, Pleuractis granulosa, Lobactis scutaria, Herpolitha limax, Sandalolitha robusta*
	Live_Massive	Acroporidae, Agariciidae, Merulinidae, Lobophylliidae Poritidae	*Diptastrea matthai, Diptastrea speciosa, Astreopora myriophthalma, Gardineroseris planulata, Hydnophora microconos, Lobophyllia hemprichii,Platygyra contorta, Platygyra ryukyuensis, Platygyra sinensis, Porites lobata, Porites solida, Porites lutea*
	Live_SubMassive	Merulinidae, Agariciidae	*Goniastrea stelligera, Pavona duerdeni, Pavona explanulata*
	NonCoral_Encrusting	Milleporidae	*Millepora platyphylla*
	NonCoral_Massive	Cardiidae, Sphenopidae, Dendrophylliidae	*Palythoa tuberculosa, Tubastraea coccinea, Tridacna gigas*
	NonCoral_SubMassive	Milleporidae	*Millepora platyphylla*
Plating	Live_Encrusting_Columnar	Merulinidae	*Hydnophora exesa, Acropora spp. (juvenile)*
	Live_Foliose	Acroporidae, Dendrophylliidae, Lobophylliidae	*Montipora aequituberculata, Turbinaria reniformis, Echinophyllia aspera*
	Live_Tabulate	Acroporidae	*Acropora spp.*
	SoftCoral_Nodular	Alcyoniidae	*Cladiella spp, Lobophytum spp, Sinularia spp*
	SoftCoral_Plating	Alcyoniidae	*Sarcophyton spp., Cryptodendrum adhaesivum*
Abiotic	Dead_Branching		See corresponding "live" category
	Dead_Collumnar		See corresponding "live" category
	Dead_Foliose		See corresponding "live" category
	Dead_Massive		See corresponding "live" category
	Dead_SoftCoral		See corresponding "live" category
	Dead_Tabulate		See corresponding "live" category
	Rubble		N/A
	Sand		N/A

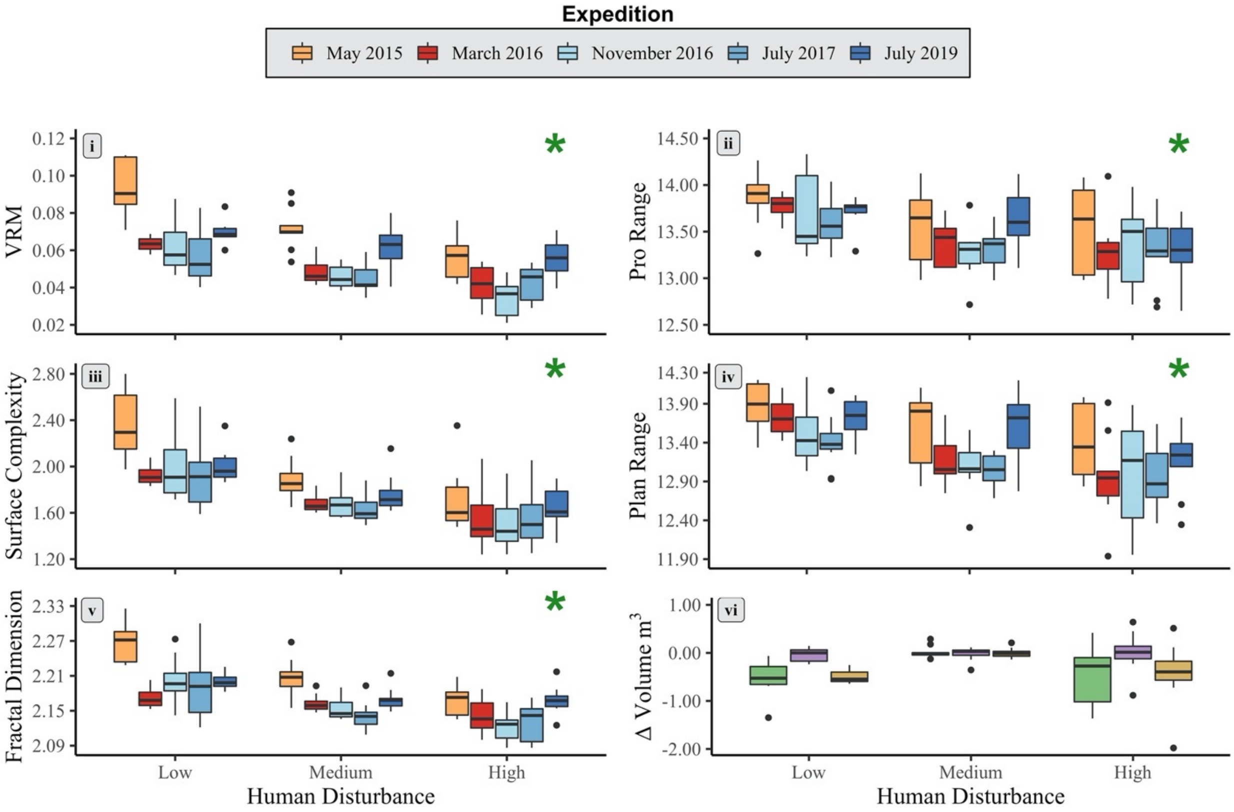

Figure A.2.1 Habitat structure metrics (i. terrain ruggedness (VRM), ii. profile curvature range, iii. surface complexity, iv. planform curvature range, v. fractal dimension, vi. habitat volume) across the local anthropogenic disturbance gradient located around Kiritimati. Metric panels i – iv are all at 1.0cm DEM resolution, with green stars indicating significance of local human disturbance.

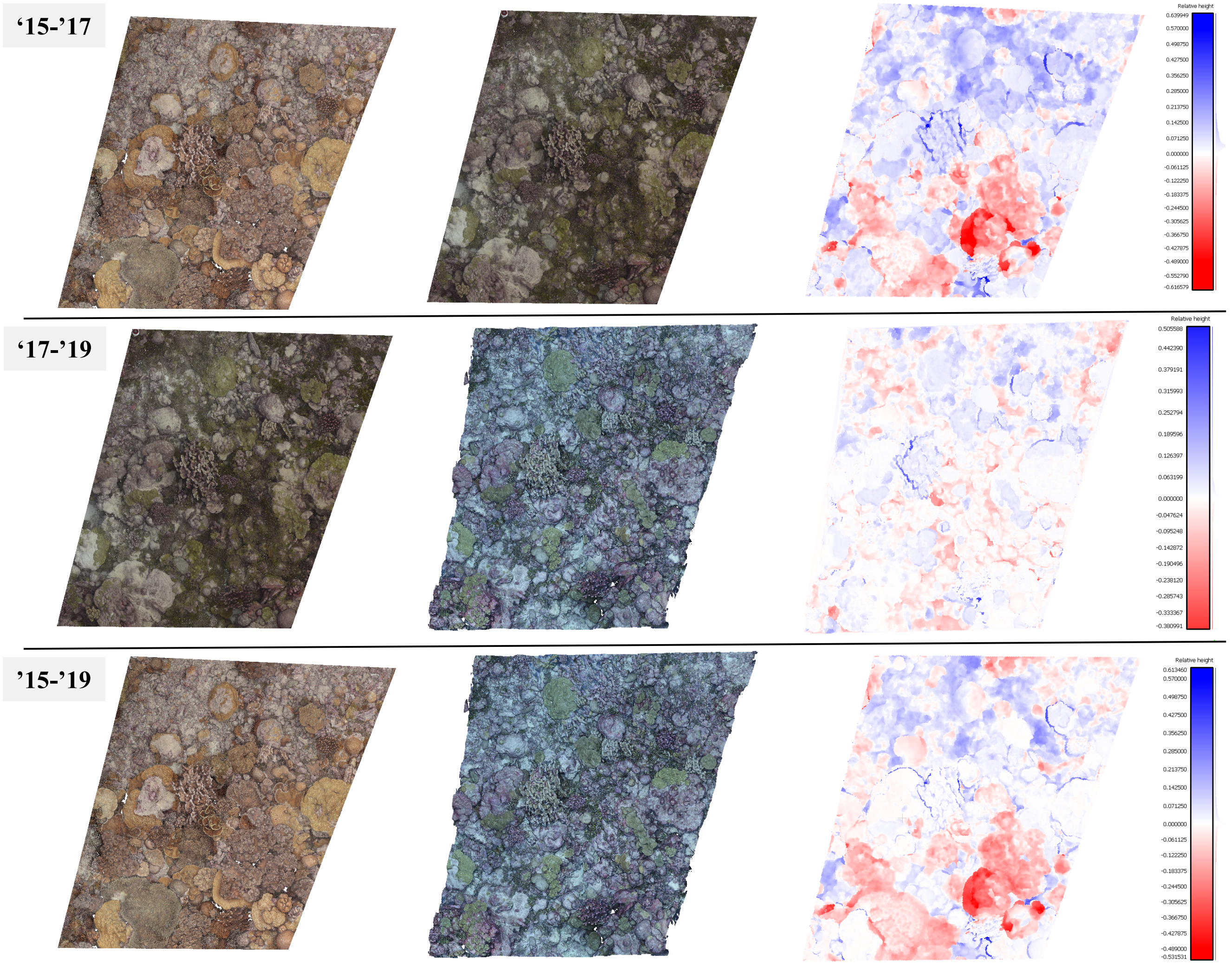

Figure A.2.2 CloudCompare volumetric change of the 3D point clouds across three time intervals: the initial two years of the study (’15-’17), the latter two years of the study (2017-2019 (’17-‘19)), and across the entire study. CloudCompare’s 2.5D volume calculation tool calculates the heigh change (m) of each point between the two point clouds and depicts the volume change as either loss (red) or gain (blue).

Figure A.2.3 Visual representation of the short-lived macroalgae phase shift within a collection of the plots around Kiritimati, with the comparison at 2015 (top) and 2017 (bottom)

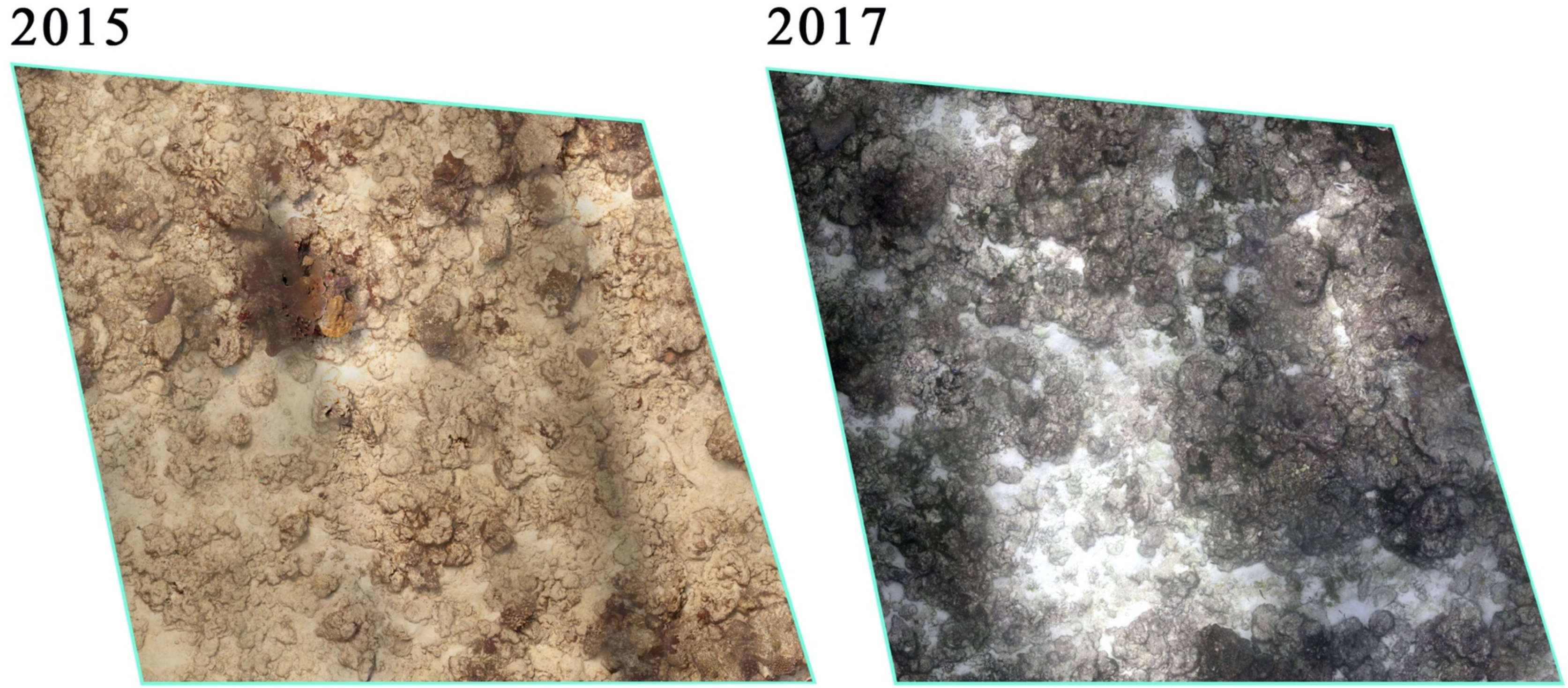

2015

2017

Figure A.2.4 Example of the rubble transport within a high disturbance plot over a two year period

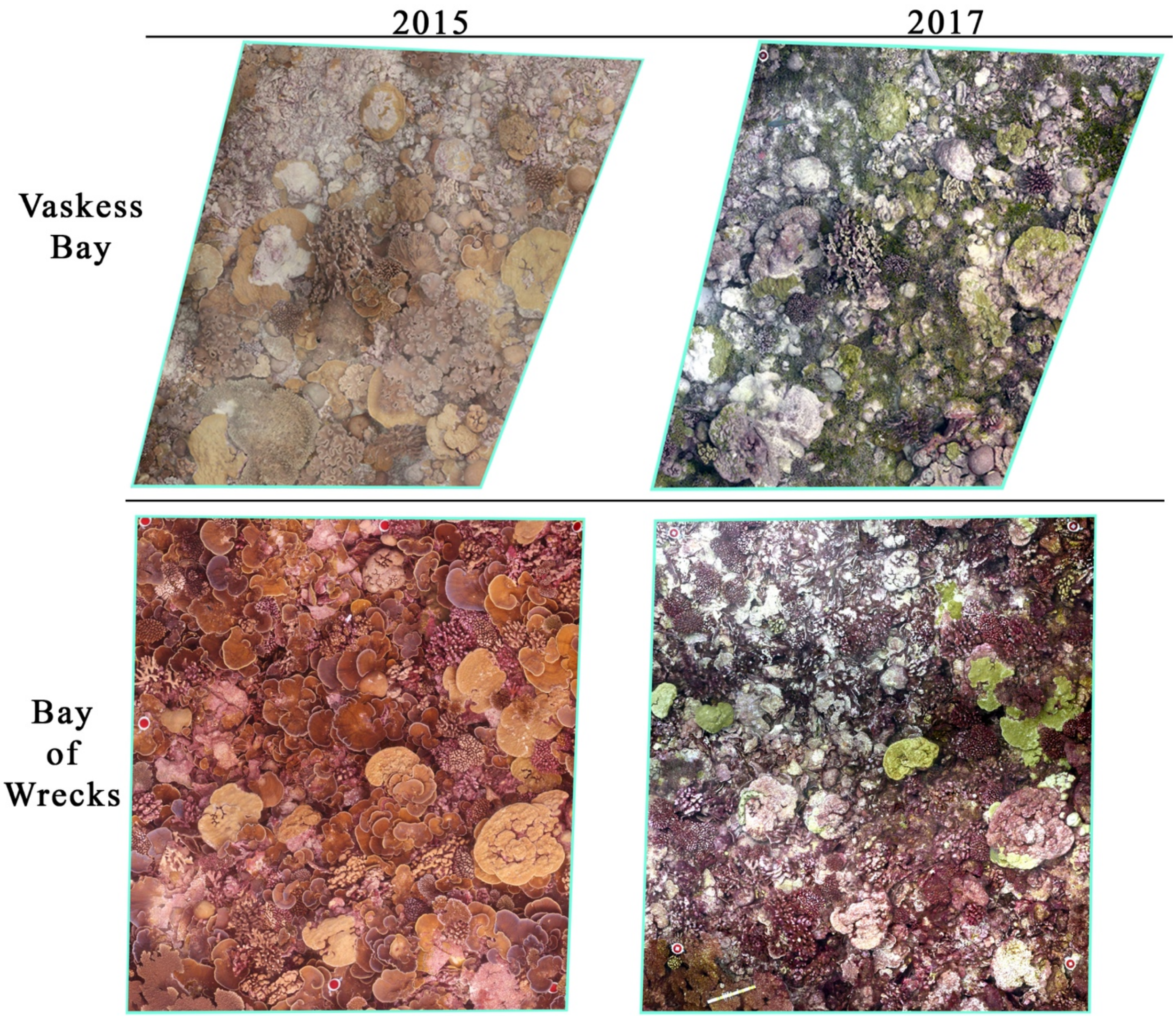

Figure A.2.5 Plot comparisons between the leeward Vaskess Bay (top row) and windward Bay of Wrecks (bottom row) regions from before the mass mortality event (2015) and 17 months post the end of the heatwave (2017).

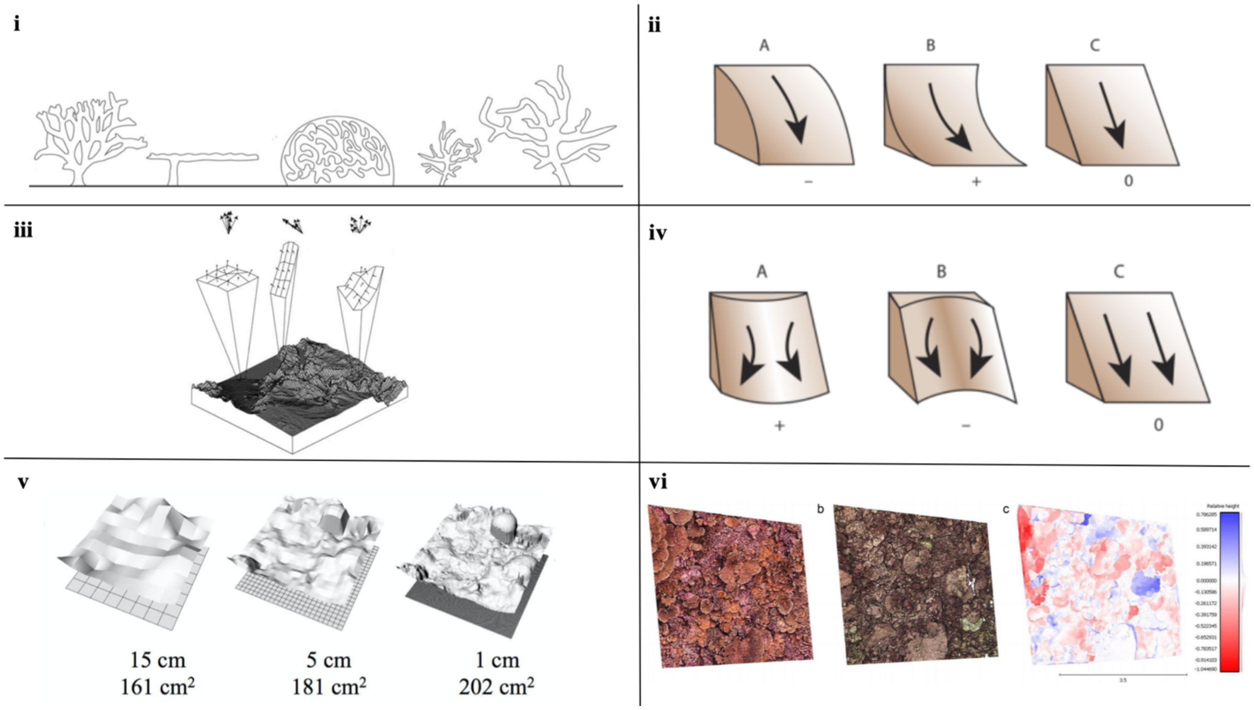

Figure A.2.6 Infographic showing the aspects of structural complexity each habitat metric captures. From top: i) surface complexity, ii) profile curvature, iii) VRM, iv) planform curvature, v) fractal dimension, vi) habitat volumetric change.

Appendix B: Random Forest top model assessment

Random forests are a machine-learning analysis used to determine top predictors for a specified response variable through the creation of a virtual forest of decision trees (Brieman 2001; Liaw and Wiener 2002; Fox et al. 2017). They are a user-friendly analysis that is able to be fine-tuned through the alteration of two parameters: 1. the *mtry* value (the number of variables used at each branch or node of a tree) and 2. The *mtree* value (the number of trees in the entire forest) (Fox et al. 2017). Many statisticians agree that the only downside of including higher-than-necessary *mtree* values is increased computational time (Prasad et al. 2006), however the debate on whether tuning the *mtry* values of the model makes significant differences is mixed. The creators of the modelling package in R and developer of the Random forest methodology state that RFs are not usually sensitive to the differences in tuned *mtry* values (Brieman 2001; Liaw and Wiener 2002), while others call for caution and state differing *mtry* values can heavily influence the outcome (Strobl et al. 2008).

B.2.1. Determining the top model classification system

For our analyses, we wished to compare complex and simple coral morphological classification systems to see which better predict the complexity and curvature metrics. A subsequent follow-up comparison was completed to see whether excluding abiotic and macroalgal cover significantly improved model variance explained for both complex and simple classifications systems. Cognizant of the debate surrounding optimally tuned parameters, we ran a comparison of each metric using default settings and optimally tuned *mtry* values, where the optimal value was determined as the number of predictors that created the least amount of out of bag error (Fig. B.2.1). To accomplish these comparisons, the percent structural cover data was first classified into a complex dataset, involving 22 distinct categories for live and abiotic morphological structure, and a simple dataset, which was comprised of five coarse categories of structure (Table B.2.1). These two datasets were duplicated and sorted into separate datasets that only contained live coral percent cover values for each morphology. This left the complex classification system with 13 categories and the simple classification system having 3 categories. Random forest regressions were then run on each of those four distinct datasets, with models trained on a randomly selected proportion of the full dataset set (66%) and validated using the remaining "test" data (34%) within the RF algorithm. This provided an output showing the amount of variance explained and total error within the final model. For all four variants, the *ntree* value was set at the default of 500 trees, as all experienced minimal error past 100-200 tree forests.

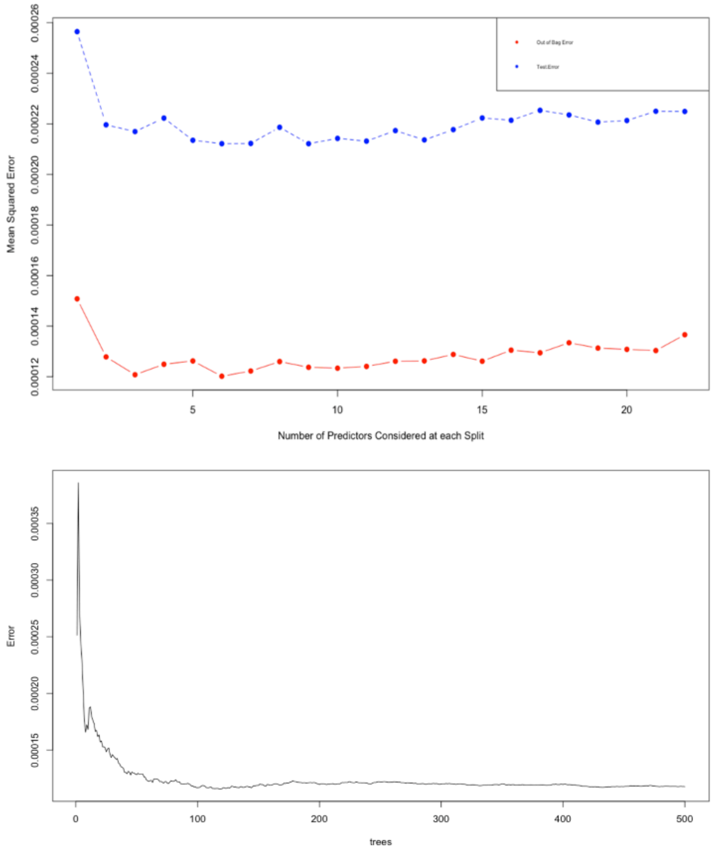

Figure B.2.1 Output plots from the RF process indicating the amount of out of bag error created when using select *mtry* values (Top) and the amount of error created in the model based on the *ntree* value (Bottom).

B.2.2 Default vs Optimal mtry settings

Overall, there were minor differences (Table B.2.1) in variance explained between the optimal and default settings. As higher *mtry* values have been shown to perform better when attempting to pinpoint a small number of important variables from a large collection of variables (Liaw and Wiener 2002), the default settings were selected to progress forward with as the majority of those reported larger default setting values.

Table B.2.1 Results from random forest model comparisons between complex ~ simple classification systems, optimal ~ default *mtry* settings, and full ~ live-only structure classifications.

Predicted Metric	**Classification System**	**Classification**	**RF parameter settings**	***ntree***	***mtry***	**Mean of squared residuals**	**Variance Explained (%)**
VRM	Complex	Full	Default	500	7	0.000119	57.18
			Optimal	500	6	0.00012138	56.41
		Live-Only	Default	500	4	0.000115	58.66
			Optimal	500	4	0.000116899	58.02
	Simple	Full	Default	500	1	0.0001533	44.94
			Optimal	500	3	0.00013874	50.18
		Live-Only	Default	500	1	0.0001533	44.43
			Optimal	500	1	0.000151	45.77
Surface Complexity	Complex	Full	Default	500	7	0.04077	49.9
			Optimal	500	3	0.0419	48.47
		Live-Only	Default	500	4	0.04432	45.55
			Optimal	500	4	0.0445	45.34
	Simple	Full	Default	500	1	0.0567	30.3
			Optimal	500	2	0.059	27.34
		Live-Only	Default	500	1	0.061	25
			Optimal	500	1	0.062	24.25
Fractal Dimension	Complex	Full	Default	500	7	0.00095	53.5
			Optimal	500	9	0.00099	51.5
		Live-Only	Default	500	4	0.00104	49.2
			Optimal	500	10	0.00107	47.59
	Simple	Full	Default	500	1	0.00133	35
			Optimal	500	1	0.001397	31.54
		Live-Only	Default	500	1	0.001324	35.12
			Optimal	500	1	0.001312	35.68
Profile Curvature Range	Complex	Full	Default	500	7	0.103	9.83
			Optimal	500	1	0.09621	15.6
		Live-Only	Default	500	4	0.103	9.7
			Optimal	500	1	0.1042	8.63
	Simple	Full	Default	500	1	0.1	12.16
			Optimal	500	1	0.1	11.99
		Live-Only	Default	500	1	0.105	7.76
			Optimal	500	1	0.1042	8.63
Planform Curvature Range	Complex	Full	Default	500	7	0.103	10.4
			Optimal	500	2	0.135	16.28
		Live-Only	Default	500	4	0.103	9.57
			Optimal	500	2	0.143	11.53
	Simple	Full	Default	500	1	0.1	17.99
			Optimal	500	1	0.1293	19.75
		Live-Only	Default	500	1	0.105	14.25
			Optimal	500	1	0.1383	14.22

B.2.3. Full vs live-coral only datasets

The exclusion of abiotic structure from the full datasets in both the complex and simple classification systems produced mixed results. Slight increases in model variance explained was noted for VRM (+1.48%) and fractal dimension (+3.40%) of the full datasets, while only fractal dimension (+0.12%) experienced an increase with the simple classification (Table B.2.1). Both curvature metrics were better explained with the inclusion of abiotic structure, which aligns with our past studies highlighting that curvature values capture changes in the underlying reefscape structure more than coral morphological structure (Fukunaga and Burns 2020). Our RF findings highlight that the abiotic structure on reefs is an important component of these metric derivations, particularly following mass-mortality events. It is hypothesized that the importance of abiotic structure became more crucial when computing the metrics of habitat structure following mass mortality events, however this wasn't examined in this study. Based on our findings, the full datasets containing abiotic structure was used in the final RF regressions reported in this study.

B.2.4. Complex vs simple classification systems

The complexity metrics explained more of the model variance in the complex classification (VRM: 12.23%; SC:19.6%; D: 18.38%) than the corresponding simple classification systems compared in this study (Table B.2.1). Curvature responded differently, with the simple classification system explaining more model variance (Pro: 2.33%; Plan: 7.59%) than the complex system, however the variance explained for either is too low to confidently say that either classification system performed better. As such, this indicates that the percent cover of various structure morphologies aren't strong predictors for either metric of curvature analyzed in this study. In conclusion, the complex classification of coral morphological structure was selected for the final model reported in this study as it outperformed the simple classification system by a significant margin.

Appendix C: Caveats of longitudinal SfM monitoring studies

This study was a continuation from Magel et al. (2019) which examined structural complexity changes before and one year after the mass mortality event. In order to add the corresponding data from an additional three expeditions, an additional 69 3D models needed to be generated. However, a few major obstacles needed to be overcome first, including accurately scaling the plots and correctly aligning the plots through time. In total, it took seven months to create all the additional 3D models in this study, with the 2016 and 2017 (those that required re-creating) models proving to be the most challenging.

C.2.1 Accurately scaling 3D Models

Ground control points are the scientific instruments used in SfM photogrammetry to accurately scale the 3D model so that accurate measurements within the model can be taken (Westoby et al. 2012; Burns et al. 2015a). Prior to 2019, all GCP's were constructed without the use of Agisoft-specific targets, which slowed down the modelling speed as a technician would have to place a marker on each target of the GCPs and validate it was placed at the marker's central point throughout the collection of images used to create the model. This additional step required patience, precision, and accuracy to place each marker correctly to keep the model error low. This process may involve any combination of placing, shifting, or removing markers that increase model error severely, to even removing photos that severely raise model error, which involves the time-consuming step of recreating the model mesh and point cloud arrangements following marker placement. The introduction by of Agisoft-specific targets in 2019 removed this time-consuming process and act as unique ID's that the software's algorithm recognizes automatically and assigns with a correct marker label at the central point of the target, thereby speeding up the modelling process and cutting down potential pathways of error.

This study faced an initial complication whereby each expedition used distinctly different apparati as GCP's, apart from a single 0.53 m PVC scale bar (Fig. C.2.1). While too small to be used accurately as a GCP or true scale bar, this PVC pipe was used as a means to "test" the accuracy of the models once the scaling was complete. Any model that didn't fall within 5% of the true length of the PVC scale bar (± 0.027m) was re-scaled and repopulated, adding on considerable amounts of time (on average, ~8hrs). The 2015 model GCP's were supplied by the MEGA lab, with all GCP's from March 2016 onwards created by the Baum Lab. March 2016 models were created following the GCP template of those used by Dr Burns in 2015, however the middle target wasn't secured on the PVC connector and was able to move when in the water. This complicated the modelling process as the digital marker for that target of the GCP needed to be placed at a spot along a known distance. For these years, it was placed manually at the intersection of the two PVC pipes of the GCP with the with the size of the 0.53m PVC pipe confirmed to be within the tolerable limits following the model scaling. November 2016 utilized photoquadrats as scaling devices, with the corner intersections acting as markers equidistantly spaced from one another. In Photoscan, a coordinate system can be setup given the geometric shape of the photoquadrat, with one corner acting as the origin (0,0) and each other corner the corresponding 1.05m away on the X and Y axes. In 2017, the same GCP was used as in March 2016, so many of the models required rescaling correctly if the 0.53m PVC pipe measurements returned lengths outside the tolerable limits. In 2019, the final year of the study, new GCP's were created using Agisoft-specific targets installed at either end, which greatly sped-up the modelling process. The distances between both targets central points were documented in the field, allowing for rapid, accurate marker placement and scaling once in Agisoft.

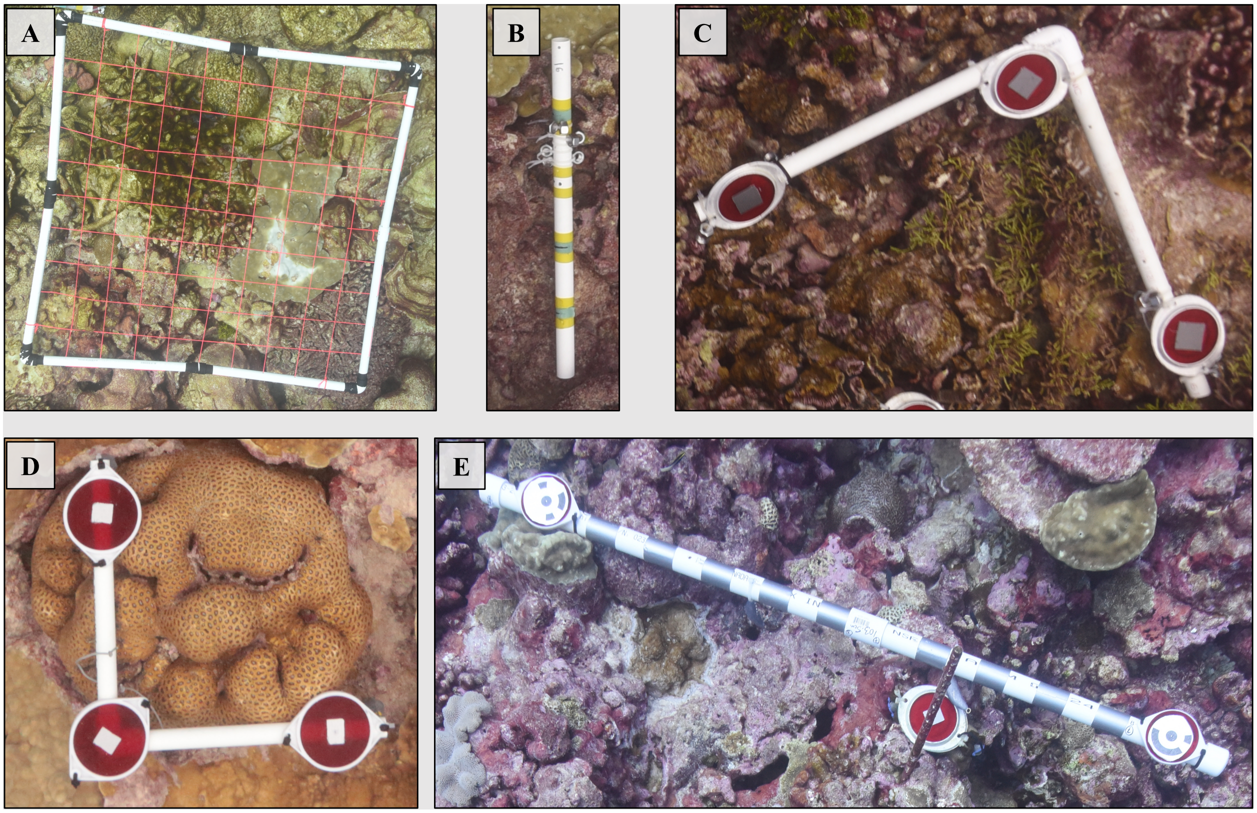

Figure C.2.1 The various GCP's used to scale the 3D plots throughout the study, including A. Photoquadrats used in the 2016a and 2016b expeditions, B. Short scale bar consistent across all expeditions within 2016-2017, C. 2017 "V-GCP", D. 2015 GCP, and E. Agisoft-target GCP's used in 2019.

C.2.2 Aligning plots through time

To date, this study is one of the few that have incorporated long-term monitoring of SfM plots. Most studies incorporating SfM photogrammetry use the methodology to either collect numerous plots along a transect as one-offs on reef structure to combine with fish or coral census data (Couch et al. 2017; Ferrari et al. 2017; Agudo-Adriani et al. 2019; Fontoura et al. 2020) or to assess the accuracy of the metrics derived through this methodology (Storlazzi et al. 2016; Fukunaga et al. 2019a; Fukunaga and Burns 2020; Torres-Pulliza et al. 2020). Few studies have used SfM as a monitoring method of reef structural complexity on the same plot through time, however those that have require establishing a permanent stake secured in the substrate to allow for repetitive sampling of the same area (Magel et al. 2019; Swirad et al. 2019). However, this is difficult to ensure given the amount of erosion reefs face each year, which may provide a rationale why so few studies have used SfM in longitudinal surveys of coral reef structural complexity. This issue was first noticed in this study when comparing plot 2D area between 2015, 2017, and 2019. This comparison indicated the sampled areas of plots differed at each timepoint, with some differences being quite drastic (±8m^2). This raised concern as altering the plot's total surface area would compound the factors at play when later examining changes in the habitat structure metrics. Upon inspection, the cause of these plot area differences was due to the fact that not all stakes were permanent and as some were lost during storms throughout the years, their replacements were placed in different locations to the original. In an effort to correct this issue, each plot was inspected through the entire duration of the study to determine which stakes remained present throughout. From there, a 16m^2 digital polygon was traced on the 2015 orthophotomosaic surface in ArcMap using the consistent stakes as corners of the digital polygon. This plot-specific shape was then re-imported for every subsequent resampling of the plot and aligned using a combination of permanent stakes present at that plot and topographical landmarks located within the plot (Fig. C.2.2). This ensured that area sampled at each plot was consistent through time comparable subsequent year's renditions of that plot when we later examined percent cover of each structural component.

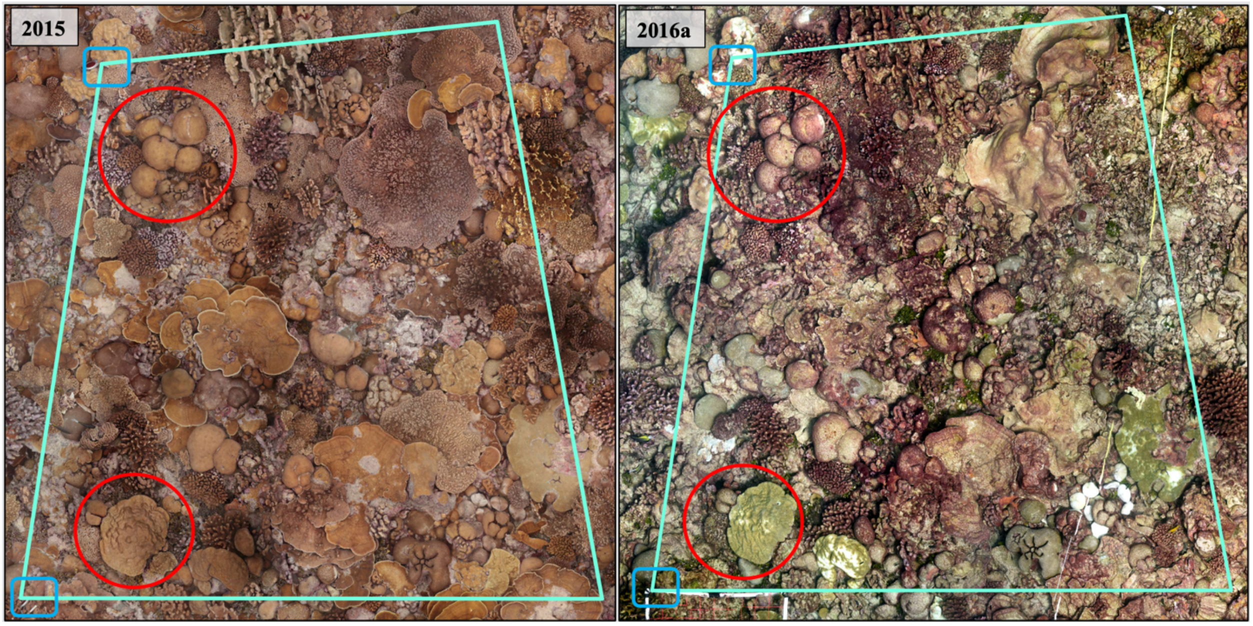

Figure C.2.2 Process of aligning PPQs based on permanent corner stakes (blue squares) and key topographical features within the plot area (red circles).